Received: 27 June 2023 | Revised: 6 September 2023 | Accepted: 6 September 2023

DOI: 10.1002/vnl.22052

RESEARCH ARTICLE

JOURNAL OF Vinyl & Additive TECHNOLOGY WILEY

A promising modified polyvinyl chloride for adsorption of boron: Preparation, adsorption kinetics, isotherm, and thermodynamic studies

Huda M. Younis[1] | **Amal A. Mohamed**[2]

[1]Department of Basic Sciences, College of Dentistry, University of Basrah, Basrah, Iraq

[2]Chemistry Department, Faculty of Science, Ain Shams University, Cairo, Egypt

Correspondence
Huda M. Younis, Department of Basic Sciences, College of Dentistry, University of Basrah, Basrah, Iraq.
Email: huda.younis@uobasrah.edu.iq

Abstract

A new promising N-methyl-D-glucamine modified polyvinyl chloride via methyl glycinate linker (PVC-MG-NMDG) was designed to extract boron from tourmaline ore from the Sikait area in the South Eastern Desert of Egypt, which assays 10.43% B_2O_3. Specifications for PVC-MG-NMDG composite were executed successfully utilizing sundry approaches, such as FT-IR, XPS, GC–MS, TGA, BET, EDX, ^{13}C-NMR, ^{1}H-NMR, ICP-OES, and XRD, which assure an acceptable synthesis of PVC-MG-NMDG. Optimized factors like pH, agitation time, primary boron concentration, composite dose, co-ions, eluting agents, and temperature have been improved. At ambient temperature, pH 9, 10 min of agitation, and 0.0138 mol/L boron ions (150 ppm), the PVC-MG-NMDG composite has a 25 mg/g maximal uptake. The extraction-distribution isotherm modeling suggests that the Langmuir model, with a theoretical value of 25.38 mg/g, more closely matches the practical value of 25 mg/g than the Freundlich model. The adsorption kinetics of boron ions by PVC-MG-NMDG were predicted with high accuracy using a pseudo-second order kinetic model, yielding a theoretical retention capacity of 27.93 mg/g. The extraction process was predicted, as shown by thermodynamic calculations, exothermic, spontaneous, and optimal extraction at low temperature; the thermodynamic factors controlling ΔS (−0.04 kJ/mol), ΔH (−13.74 kJ/mol), and ΔG values rise from −1.82 kJ/mol at 298 K to −0.19 kJ/mol at 338 K. Boron ions can be eluted from the overloaded composite by 0.5 M H_2SO_4 with a 95% efficiency rate. It was established that PVC-MG-NMDG composite reveals a worthy separation factor to most co-ions and gives a good separation power. Boric acid with a boron content of 17.23% and purity of 98.56% can be obtained through alkali fusion with NaOH flux and subsequent adsorption using a PVC-MG-NMDG composite.

Highlights

- A New modified polyvinyl chloride (PVC-MG-NMDG) was successfully prepared.
- The characteristics of new composite were verified via different techniques.

Huda M. Younis and Amal A. Mohamed contributed equally to this study.

- The new composite reached its maximum boron absorption of 25 mg/g at 25°C.
- The extraction as an exothermic, spontaneous process at low temperature.
- The new composite has been applied to a real sample of Sikait tourmaline ore.

KEYWORDS

boron recovery, Egypt, methyl glycinate, N-methyl-D-glucamine, polyvinyl chloride, Sikait area, south Eastern Desert, tourmaline ore

1 | INTRODUCTION

Boron is an abundant trace element found in both the water and rocks of our planet. Boron is an element that can be found in the planet's lithosphere; it is typically found in soil and rocks and has an average concentration of 10 mg/kg in the earth's crust, making up only 0.001% of the earth's elemental composition. Its concentration in groundwater ranges from 0.3 to 100 mg/L, whereas in seawater, it averages around 4.5 mg/L in the hydrosphere.[1–3] Its properties lie between those of metals and nonmetals, and in some ways, it even mimics its metal- and nonmetal-neighbors, aluminum, carbon, and silicon. Boron's electron structure predicts that it will most frequently form three bonds. There is also a considerable propensity for a fourth bond to be formed, bringing the total number of bonds to eight, and completing the octet of valence electrons. Boron has never been found in nature as a pure element. However, it is more commonly found in the form of boric acid ($B(OH)_3$ or H_3BO_3) and its salts (borates) or as borosilicate.[4,5]

Boron and its compound assortments are widely employed in multiple industries, like electronics, glass, porcelains, catalysts, ceramics, leathers, semiconductors, pharmaceuticals, cosmetics, insecticides, fuels, and cleaning derivatives. Most of the world's boron compounds or products are utilized in the glass sector, which accounts for more than half of all consumption.[6,7] In addition, boron-10 isotopes and boron carbide alloys are vital in the nuclear sector because they can regulate the rate of a nuclear reaction, preventing an explosion.[8–10]

To recover boron from different mediums via different procedures, are functionalized. Solvent extraction (sx), ion-exchange (IX) and adsorption,[11] reverse osmosis (RO),[12] electrocoagulation,[13,14] ion-exchange membranes,[15] Donnan dialysis,[16,17] chemical coagulation,[18,19] and hybrid processes[20] are applied. In the field of hydrometallurgy, solvent extraction is a typical method for the recovery of key metals. The feed solution, extraction solvent, shake time, aqueous and organic phases in the extraction process, stripping stages, and so forth. all have a role in determining the efficiency of solvent extraction. In the SX process, the extractant occupies a key role.

Numerous extractants have been tried and tested in prior research for use in the solvent extraction method of boron extraction. Proper agent selection is essential for effective solvent extraction. Boron's well-known propensity to create stable esters with poly-hydroxylated organics (e.g., saccharides, poly-alcohols) is also used in the separation process.[21] Particularly robust complexes are generated when poly-alcohols are utilized, with the hydroxyl groups (OH) oriented in such a way as to exactly meet the structural characteristics required by tetrahedrally-coordinated boron (Scheme 1). It must be emphasized that the proton becoming free in the solution results from complexation (Equation 1). This suggests that a pH buffer is required to prevent ester hydrolysis in an acidic environment. It is common practice to classify boron extraction agents as either mono-hydroxy alcohols (2-butyl-1-n-octanol),[22–24] di-hydroxy alcohols (diols),[25,26] or phenols.[27] Alcohols with 8–12 carbon atoms, such as 2-ethyl-1,3-hexanediol (EHD),[28] 2-butyl-2-ethyl-1,-3-propanediol (BEPD),[29,30] and 2,2,4-trimethyl-1,3-pentanediol,[31] have been shown to have excellent boron extraction efficiencies.

$$\begin{aligned} &B(OH)_3 + 2R(OH)_2 \rightleftharpoons \left[B(RO_2)_2\right]^- + 3H_2O \\ &+ H^+ \text{with } R(OH)_2 \\ &= \text{generic di-alcohol} \end{aligned} \quad (1)$$

Chelating resin, a typical technique for extracting boron from solutions, appears to be one of the most efficient techniques.[32] Excellent selectivity to boron has been shown by chelating resins with ligands containing three or more extra hydroxyl groups positioned in the cis-position, the so-called "Vis-diols".[33] The selective sorption properties of these ion exchangers (resins) can be attributed to processes using boron. Boric acid esters of borate anion complexes or boron with a proton as the counter ion are common ways for polyoxide compound molecules to bind together.[34] According to the findings that were gathered, the occurrence of a tertiary amine

SCHEME 1 Schematic drawings of borate esters complexes.

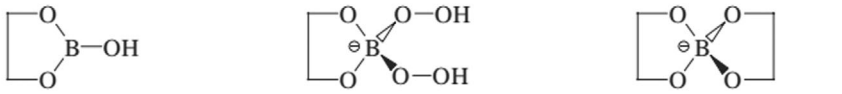

group appears to be essential for boron chelation. It does this by recapturing the proton that is released when borate is complexed by hydroxyl functionalities.[35] As a result of these discoveries, research into the development of B-selective resins has been initiated.[36] The majority of the synthetic resins were produced by modifying a copolymer made of styrene and divinyl benzene with N-methyl-D-glucamine (NMDG) and combining it with other solid supports like cellulose.[37,38] To make a coordination complex, the efficient groups of these ion exchangers (resins) use a covalent bond to bind boron to themselves, therefore capturing the element.[39]

Over the past two decades, scientists have focused on learning how to synthesize boron-selective resin with functions other than NMDG. The glycidyl-modified and sorbitol-grafted resins are based on cross-linked polystyrene.[40–42] Diallyl amine-modified terpolymers of glycidyl methacrylate, methyl methacrylate, and ethylene glycol dimethacrylate (GMA/MMA/EGDMA),[43] hybrid gels made from TEOS and 3-glycidoxypropyltrimethoxysilane (GPTMS), and GPTMS and N-methyl-D-glucamine as precursors,[44] The solid silica backing was altered with NMDG[45,46] and activated carbon anchored by salicylic acid.[47,48]

The main objectives of this study are to design a new composite (PVC-MG-NMDG), with high chemical, thermal stability and high affinity and selectivity towards boron ions. This composite is employed for boron extraction from both synthetic and real samples. Characterized the new PVC-MG-NMDG via different tools were done successfully. The loading and elution factors were enhanced. Physico-chemical aspects investigate the thermodynamics, equilibrium, and kinetics of boron extraction from a tourmaline ore sample from the Sikait area in the South Eastern Desert of Egypt, which assays 10.43% B_2O_3.

2 | MATERIALS AND METHODS

2.1 | Instrumentation

All samples were weighed using an analytical balance of type Sartorins TE 214S having a maximum sensitivity of 10^{-5} g. The hydrogen ion conc. was measured using a digital pH meter of the type Digimed DM-21 (Japan) with an error of ±0.1. For the equilibrium experiments, a known weight of PVC-MG-NMDG composite and a definite volume of boron bearing leach liquor were shaken using Vibromatic-384 shaker. The quantitative analysis of boron was carried out by a single beam spectrometer, Meterch Inc. (SP-8001) using violet-blue carmine indicator at 615 nm against proper standard solution,[49] the molar absorptivity of the B-carmine complex in 92% H_2SO_4 is 5.5×10^3 ($a = 0.51$). ICP-OES (Prodigy High Dispersion ICP, TExxLEDYNE-Leeman Labs USA) was used to make specification of the resulted boron concentrate and to determine the tolerance limit of the co-exist ions. X-ray diffraction (XRD) technique, PHILIPS PW 3710/31 diffractometer, scintillation counter, Cu-target tube and Ni filter at 40 kV and 30 mA were used. IR spectra were recorded by FT-IR 4100 Gasco-Japan spectrometer, using KBr disks. ^{1}H, ^{13}C-NMR spectra were made by mercury 400 Bruker spectrometer and recorded at 400 MHz. Spectroscopic analysis was performed at 293 K on diluted solution using DMSO solvent. Chemical shift (δ) is reported in ppm and coupling constant (J) is reported in Hertz (Hz). GC–MS analyses were performed using GC–MS analyses were performed using Shimadzu Qp-2010 Plus spectrophotometer. The thermal stability was studied using thermo-gravimetric analyses (TGA), carried out in a nitrogen atmosphere using (Shimadzu TGA-50 Model) thermal analyzer. X-ray photoelectron spectroscopy (XPS) experiments were carried out using a Kratos Axis Ultra spectrometer (Kratos, Manchester, UK). A 225 W monochromatic aluminum source (Alkα) was used. The elemental analysis of boron concentrate product and PVC-MG-NMDG composite were recorded using EDX (JSM–7900F, Jeol, Tokyo, Japan).

2.2 | Reagents

All chemicals were manufactured with high-purity chemicals suitable for analytical usage. Polyvinyl chloride (PVC), N-methyl-D-glucamine, and methyl glycinate hydrochloride were all provided by Sigma-Aldrich Inc. The Polish company POCH S.A. provided HCl, HNO_3, H_2SO_4, and NaOH of analytical quality. Both the boric acid and the carminic acid came from a town called Merch in Germany. The alcohol, DMF, ethyl acetate, and dimethyl sulfoxide came from Fluka in England.

All solvents used were freshly distilled after undergoing the standard laboratory purification procedures. Fire-dried glassware was utilized for all reactions. Paper chromatography (PC) was the means of checking the reaction's progress. The eluent is a 50/50 mixture of ethanol and ethyl acetate. A UV lamp was utilized to see the computer's spots.

2.3 | Experimental steps

The appropriate weight of 5.717 g of $B(OH)_3$ was liquefied in 1000 mL of pure distilled water to produce a 1000 mg/L (0.092 mol/L) boron standard stock solution, which can be further diluted to 150 mg/L (0.0138 mol/L). In contrast, various standard solutions containing 1000 ppm of potential co-existing ions throughout boron extraction by PVC-MG-NMDG chelating compounds have been created by mixing 1000 milliliters of distilled water with an appropriate amount of their salts.

2.4 | The extraction steps

Boron extraction from a synthetic solution using a PVC-MG-NMDG chelating composite was optimized by adjusting the following factors: pH, agitation time, beginning B concentration, PVC-MG-NMDG dose, temperature, and the concentrations of various co-ions. These assays involved mechanically swirling 25 mL of a 150 mg/L synthetic B solution with varying concentrations of PVC-MG-NMDG over a set time at four different temperatures, with the stirring speed set at 200 rpm. Using Equation (2), we determined the maximal absorption capacity (q_{max}) in mg/g and the distribution coefficient (K_d) to evaluate the efficacy of the boron extraction procedure[50]:

$$q_{max} = (C_o - C_e) \times \left[\frac{V}{m}\right] \quad (2)$$

where C_0 and C_e are the concentrations of boron (mg/L) at the initial and end of the reaction, V is the volume of the solution containing boron, and m is the weight of the dry PVC-MG-NMDG composite (g). K_d, the distribution coefficient, is determined in the meantime by plugging V, the volume of the liquid phase (mL). The dispersion coefficient was calculated using Equation (3)[51]:

$$K_d = \frac{C_o - C_e}{C_o} \times \left[\frac{V}{m}\right] \quad (3)$$

3 | RESULTS AND DISCUSSION

3.1 | Synthesis of a polyvinyl chloride-supported N-methyl-D-glucamine (PVC-MG-NMDG) composite

Polyvinyl chloride-reinforced N-methyl-D-glucamine (PVC-MG-NMDG) composite was synthesized via three vital stages. The first neutralization stage begins by refluxing a mixture of 0.1 mole (≈12.5 g) of methyl glycinate hydrochloride and 0.1 mole of NaOH (4 g) in an appropriate 50 mL of absolute ethanol as a diluent. At a temperature of 50°C, the mixture was allowed to reflux for 2 h. The chief goal of the neutralization stage is to increase the nucleophilicity of methyl glycinate hydrochloride towards PVC. The mixture is cooled to ambient temperature when the condensation reaction has been completed. A white precipitate was obtained after three washes in 100% ethanol, precipitate formation using vacuum air Buchner, and drying at 50°C for 3 h.

The second nucleophilic substitution step begins by adding 0.16 mole of neutralized methyl glycinate (7.1 g) to 0.16 mole of PVC (5 g) and 0.16 mole of NaOH (3.2 g) in a condenser in an appropriate 100 mL of DMF as a diluent for 6 h at 100°C. Finally, the third nucleophilic substitution step was carried out by adding the later mixture to 0.1 mole (19.5 g) of N-methyl-D-glucamine, and the mixture was refluxed for 5 h at 100°C. The working reaction progress was monitored by thin-layer PC via PC sheets with ethanol and ethyl acetate as solvents. A UV lamp was utilized to see the spots. After the reaction was complete, we retrieved the product by allowing it to cool. We then washed it in 100% absolute ethanol three times to eliminate any residual DMF and other reaction byproducts. Afterward, the PVC-MG-NMDG composite, with a density of around 1.46 g/cm^3, was produced by drying the resulting precipitate in a furnace at 110°C for 3 h. The synthesis of a polyvinyl chloride-supported N-methyl-D-glucamine (PVC-MG-NMDG) composite and the recommended reaction mechanism were exemplified in Scheme 2. A proposed chelation mechanism for boron by PVC-MG-NMDG composite is illustrated in Scheme 3, which indicates a suggested two modes of chelation. In the first mode of chelation, 1 mole of boron ion was coordinated by 2 mole of the composite through the two vicinal –OH groups, while in the second mode of chelation, 1 mole of boron ions was coordinated by 2 mole of the composite. From the two modes of chelation, it was noticed the formation of five membered ring containing boron, giving enhanced stability to the final chelate.

(A) ***First neutralization step:***

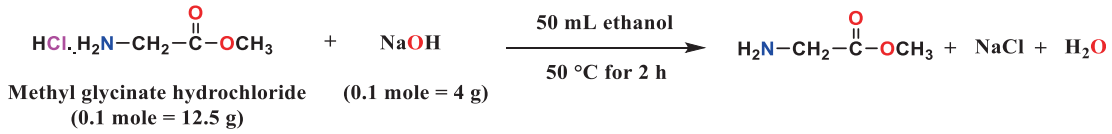

(B) ***Second nucleophilic substitution step:***

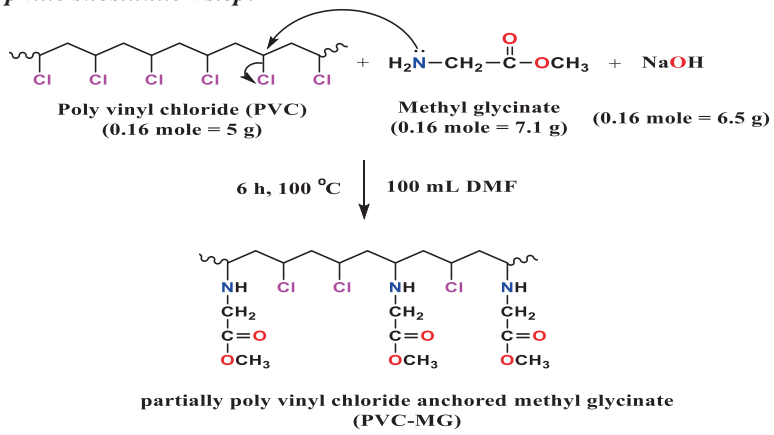

(C) ***Third nucleophilic substitution final step:***

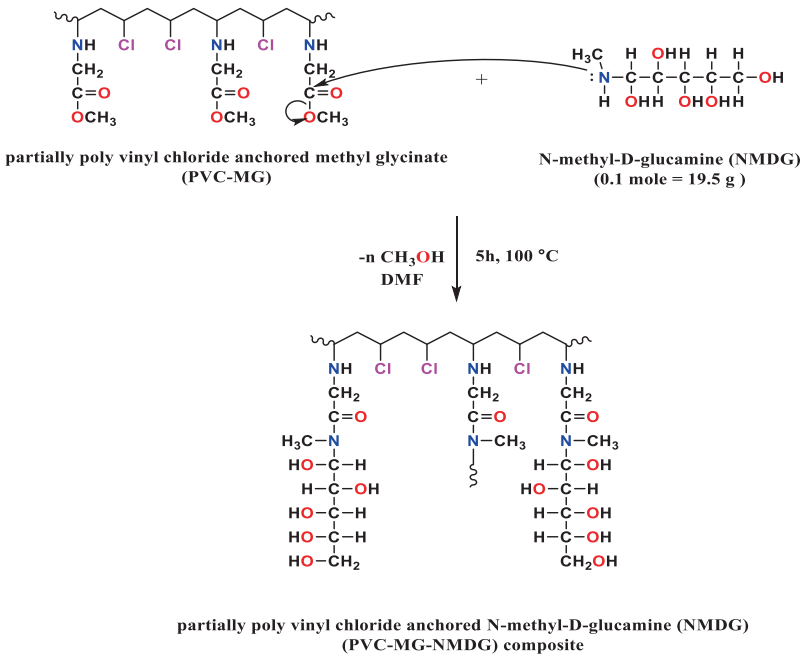

SCHEME 2 Synthesis of partially polyvinyl chloride anchored N-methyl-D-glucamine (PVC-MG-NMDG) composite.

3.2 | Specification of polyvinyl chloride supported N-methyl-D-glucamine (PVC-MG-NMDG)

The product profit was establish to be ≈13 g; m.p ≈ 235–250°C; FT-IR (KBr) ν/cm^{-1} = 3550 (–OH), 2853 (–CH aliphatic), 701.38 ($(-CH_2)_n$ aliphatic), 1686 (–C=O), 1339 (–C–O), 1250 (–C–N), 3300 (–NH), 636 (–C–Cl) and 661, 750 (C–B–O). ^{1}H-NMR (400 MHz, 25°C, DMSO-d_6, TMS) δ, ppm: 1.83 (d, 2H, $(-CH_2)_n$, J = 12.81, 5.94 Hz), 4.06 (m, H, $(-CHCl)_n$, J = 5.95 Hz), 2.88 (m, H, –CH–N–, J = 5.32, 4.61 Hz), 3.87 (m, –NH, J = 5.53 Hz), 3.49 (d, 2H, $-CH_2$, J = 5.53 Hz), 2.89 (s, 3H, $-N-CH_3$, J = 5.12 Hz), 3.83 (m, 1H, –CH–OH, J = 9.12, 5.96 Hz), 6.27 (m, 1H, –CH–OH, J = 5.9 Hz), 4.76 (m, 1H, $-CH_2-$OH, J = 5.96 Hz). ^{13}C-NMR (100 MHz, 25°C, DMSO-d_6,

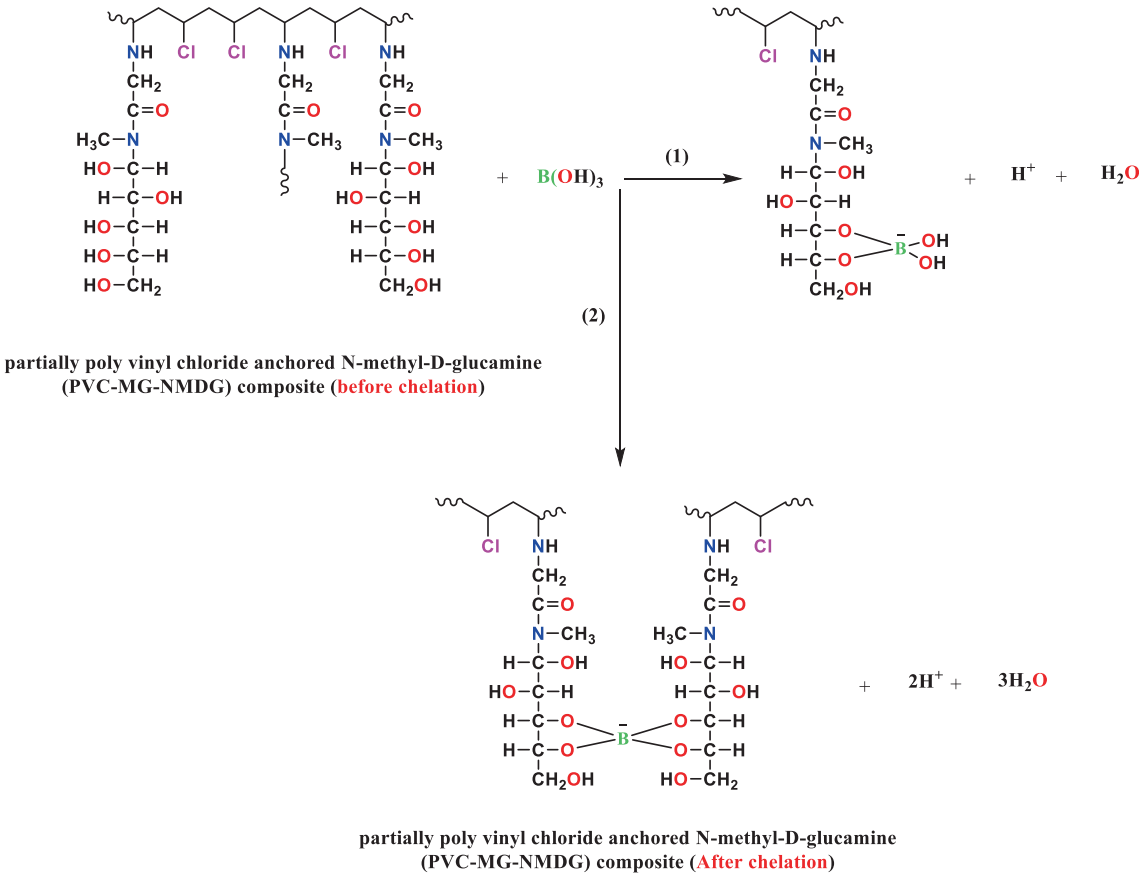

SCHEME 3 A recommended mechanism for boron chelation by PVC-MG-NMDG composite.

TMS) δ, ppm: 29.7 (s, –N–$\underline{C}H_3$), 57.5 (s, –$\underline{C}$H–Cl), 39.7 (s, (–$\underline{C}H_2)_n$), 45.3 (s, –$\underline{C}$H–N), 50.7 (s, –$\underline{C}H_2$), 64.2 (s, –$\underline{C}H_2$OH), 72.2 (s, –$\underline{C}$HOH), 170 (s, –$\underline{C}$=O). GC–MS (EI, 30 eV), m/z (% rel): $[m/z]^+$ of 264, 62, 125, 43, 18, 36, 15, 17, 78, 92, 106, 156, 128, 32, 46, 181. Anal. Calc. for $[C_{10}H_{20}N_2O_6]_n$ building unit (264.35 g/mol, $n = 1$): C, 45.39; H, 7.56; N, 11.34; O, 36.31. Found: C, 45.31; H, 7.6; N, 11.31; O, 36.33.

3.2.1 | Infrared analysis

Fourier transform infrared (FTIR) spectroscopy, was utilized to make important predictions about the occurrence of functional groups in the produced PVC-MG-NMDG composite. The chief assignments in the manufactured PVC were considered as 2853, 2911, and 2969 cm^{-1} (–CH aliphatic), 701.38 cm^{-1} ($(CH_2)_n$ aliphatic), and 606, 636, and 682 cm^{-1} (–C–Cl). After condensation of PVC with methyl glycinate to form PVC-MG, new assignments were observed, such as 3300 cm^{-1} (–NH), 1250 cm^{-1} (–C–N), 1756 cm^{-1} (–C=O of ester), and 1090 and 1339 cm^{-1} (–C–O of ester). Moreover, the condensation between PVC-MG and N-methyl-D-glucamine (NMDG) will form a PVC-MG-NMDG composite and construct a shift to a lower frequency that is observed with the amide carbonyl at 1686 cm^{-1} (–C=O of amide), and the vanishing of 1090 and 1339 cm^{-1} (–C–O of ester). It is expected that the critical vibrational tasks were attended at 3550 cm^{-1} of the vicinal –OH groups of PVC-MG-NMDG, which must vanish after boron chelation. However, it just did not happen, as a reasonable number of (OH) without chelation with boron were still present. The further assignments of PVC-MG-NMDG that persisted unmoved after chelation with boron were 701.38 cm^{-1} ($(CH_2)_n$ aliphatic), 2853, 2911, and 2969 cm^{-1} (–CH aliphatic), 606, 636, and 682 cm^{-1} (–C–Cl), 3300 cm^{-1} (–NH), 1250 cm^{-1} (–C–N), 1686 cm^{-1} (–C=O of amide), and 3550 cm^{-1} (–OH). The spectrum of PVC-MG-NMDG with boron is shown in Figure 1. The arrival of innovative bands in the chelate at 750 and 661 cm^{-1} may be correlated with making a coordinated C-B-O bond.[12,28]

3.2.2 | X-ray photoelectron spectroscopy analysis

The chemical compositions of unmodified PVC, PVC-MG, PVC-MG-NMDG, and PVC-MG-NMDG-B were

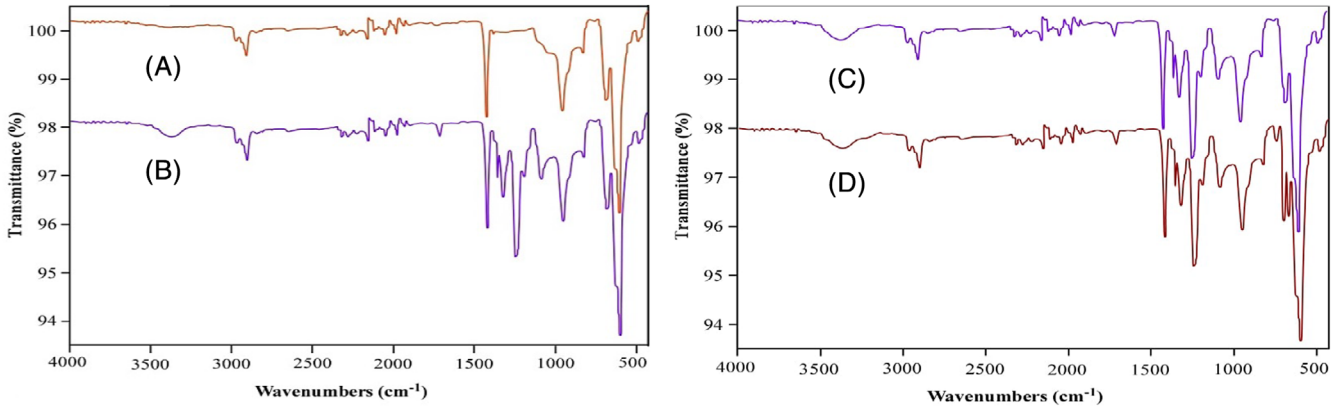

FIGURE 1 Fourier transform infrared spectra of (A) unmodified PVC; (B) PVC-MG; (C) PVC-MG-NMDG; (D) PVC-MG-NMDG-B.

inspected by XPS, as revealed in Table 1 and Figure 2. The (4) solid samples constrained C_{1S} and Cl_{2P}, which match the peaks at 287.14 eV (carbon content is 37.82%) and 202.31 eV (chlorine content is 55.87%), respectively.[52] Compared with PVC, the PVC-MG showed an increase in carbon content to 41.62%, the appearance of new assignments at 405 and 542 eV due to the presence of N_{1S} and O_{1S},[53] and finally, a decrease in the content of chlorine from 55.87% to 27%, which reflects the successful partial amination of PVC by methyl glycinate to give PVC-MG with anchoring efficiency of 51.67%. Furthermore, compared with PVC, the PVC-MG-NMDG showed an increase in both nitrogen and oxygen contents from 10.28% to 13.11% and 14.77% to 19.1%, respectively, also indicating a good amination of PVC-MG by N-methyl-D-gluconate. After a successful amination of PVC by both methyl glycinate and N-methyl-D-gluconate, the chelation of boron by PVC-MG-NMDG for boron chelate was assigned a frequency of 191 eV, which is due to the presence of B_{1S} with a boron content of 1.37%.[54] So, it can be settled that the chemical amendment of PVC with both methyl glycinate and N-methyl-D-gluconate to form the PVC-MG-NMDG composite is a successful process.

3.2.3 | Brunauer–Emmett–Teller (BET) analysis

The Brunauer–Emmett–Teller (BET) was exploited to display the N_2 loading and desorption on PVC, PVC-MG, and PVC-MG-NMDG. From Table 2, the specific pore volume V ($cm^3\ g^{-1}$), surface area σ_{BET} ($m^2\ g^{-1}$), and average pore diameter d (nm) of PVC were 0.0021 $cm^3\ g^{-1}$, 0.27 $m^2\ g^{-1}$, and 6.59 nm.[55] When amination was performed by methyl glycinate to form PVC-MG, the pore volume and surface area increased to 0.248 $cm^3\ g^{-1}$ and 170.8 $m^2\ g^{-1}$, while the diameter of the typical pore (average pore diameter) decreased to 5.56 nm. Moreover, the condensation reaction between PVC-MG and N-methyl-D-gluconate resulted in the formation of a PVC-MG-NMDG composite with an enhancement in both specific pore volumes (0.319 $cm^3\ g^{-1}$) and surface area (217 $m^2\ g^{-1}$), while vanishing in average pore diameter to 4.73 nm. The average pore diameters of 5.65 and 4.73 nm for both PVC-MG and PVC-MG-NMDG, respectively, indicated that they were in the mesoporous region. These results proved the effective reactions of PVC to PVC-MG and PVC-MG-NMDG composite. The surface area σ_{BET}, specific pore volume V, and average pore diameter d of PVC, PVC-MG, and PVC-MG-NMDG were illustrated in Table 2.

3.2.4 | SEM–EDX analysis

The surface morphology of PVC, PVC-MG, PVC-MG-NMDG, and PVC-MG-NMDG-B were checked by SEM analysis at 3000× enlargement with 5 μm of full scale and energy of 15 Kev. It was found that PVC was comprised of a smooth and sleek micro-structure. After condensation of PVC to PVC-MG, it was establish that the surface morphology was twisted to be more dotted and unevenness. After converting PVC-MG to PVC-MG-NMDG, an irregular and sinuous networking micro-structure was observed. When boron ions were introduced to PVC-MG-NMDG, the surface was converted to be more irregular, sinuous networking micro-structure and roughness due to boron ions extraction onto the surface. The chemical verification of PVC, PVC-MG, PVC-MG-NMDG, and PVC-MG-NMDG-B by EDAX analysis were donated C, Cl for PVC, C, Cl, O, N for PVC-MG and PVC-MG-NMDG, and C, Cl, O, N, B for PVC-MG-NMDG-B. These observations confirmed the successful synthesis of PVC-MG-NMDG composite from PVC and its capability to extract boron ions (Figure 3A–D).

Sample	C_{1S}, %	O_{1S}, %	N_{1S}, %	Cl_{2P}, %	B_{1S}, %
PVC	37.82	—	—	55.87	—
PVC-MG	41.62	14.77	10.28	27	—
PVC-MG-NMDG	35.85	19.1	13.11	25.5	—
PVC-MG-NMDG-B	35	18.3	12.7	25	1.37

TABLE 1 Chemical composition of PVC, PVC-MG, PVC-MG-NMDG, and PVC-MG-NMDG-B.

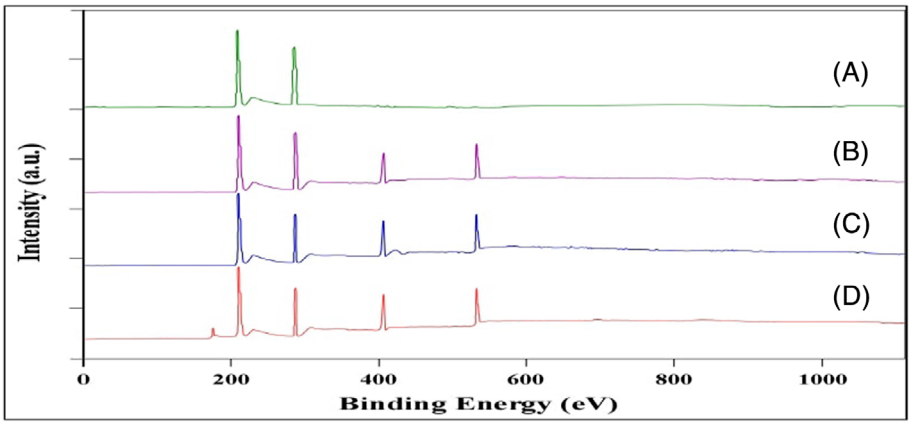

FIGURE 2 X-ray photoelectron spectra of (A) PVC, (B) PVC-MG, (C) PVC-MG-NMDG, (D) PVC-MG-NMDG-B.

TABLE 2 The surface area σ_{BET}, specific pore volume V, and the average pore diameter d, of PVC, PVC-MG, and PVC-MG-NMDG.

Sample	σ_{BET}, $m^2\ g^{-1}$	V, $cm^3\ g^{-1}$	d, nm
PVC	0.27	0.0021	6.59
PVC-MG	170.8	0.248	5.65
PVC-MG-NMDG	217	0.319	4.73

3.2.5 | TGA investigation

A TGA examination is used to inspect the influence of the chemical variation on the thermal stability of PVA. Figure 4 depicts the TGA thermographs of the PVC, PVC-MG, PVC-MG-NMDG, and PVC-MG-NMDG-B from room temperature to 800°C with a heating grade of 10°C min^{-1}. The TGA stages, deflection temperature, weight loss percentage, and final weight residue are revealed in Table 3.

From TGA fallouts, five inflections were observed. A primary mass loss of 5% was observed for PVC, PVC-MG, PVC-MG-NMDG, and PVC-MG-NMDG-B samples as soon as the temperature roughly reached 102°C. This loss is owing to the evaporation of physically weak and chemically strongly bound H_2O, as shown in Table 3.[56] After 102°C, a variance was detected among the PVC and the further samples. For the unchanged PVC, inflections were experienced from 102 to 265°C (weight loss of 9%), 265–465°C (weight loss of 72.5%), and 465–800°C (weight loss of 13%), which corresponded to three distinct decomposition steps with a final char residue of 2.5%. The great weight loss of 72.5% at 265–465°C may be assigned to the side chain polyene and cyclization reactions due to the dehydrochlorination of PVC and HCl getting out of the PVC polymer chain, while the temperature of 465–800°C (weight loss of 13%) may be related to the breakdown and carbonization development; additionally, the third stage can be coordinated to the thermo-oxidation development.[57] Like in PVC, inflections were observed for PVC-MG: 102–210°C (weight loss of 18%), 210–460°C (weight loss of 25%), 460–600°C (weight loss of 45%), and the presence of a final weight remainder stage of 7% weight loss at 600–800°C, which may be due to the increase in the organic components, which represents the methyl glycinate.

PVC-MG-NMDG indicated the occurrence of inflections at 105–235°C (weight loss of 23%), 235–510°C (weight loss of 40%), 510–600°C (weight loss of 22%), and the presence of a final weight residue stage of 10% weight loss in the variety between 600 and 800°C. The shift of the further deflection temperature ought to be correlated to the successful incorporation of N-methyl-D-glucamine onto the PVC-MG matrix, which causes thermal stability and enhancement of the final char residue to 10%.

Moreover, PVC-MG-NMDG-B also exposed the occurrence of inflections at 102–297°C (weight loss of 21%), 297–575°C (weight loss of 28.5%), 575–600°C (weight loss of 30.5%), and the final high-weight char stage of 15% weight loss, which may result in the formation of both residual boron oxide and char residue. The shift to a higher degradation temperature, 297°C, which is higher than the later, must be interrelated to the effective

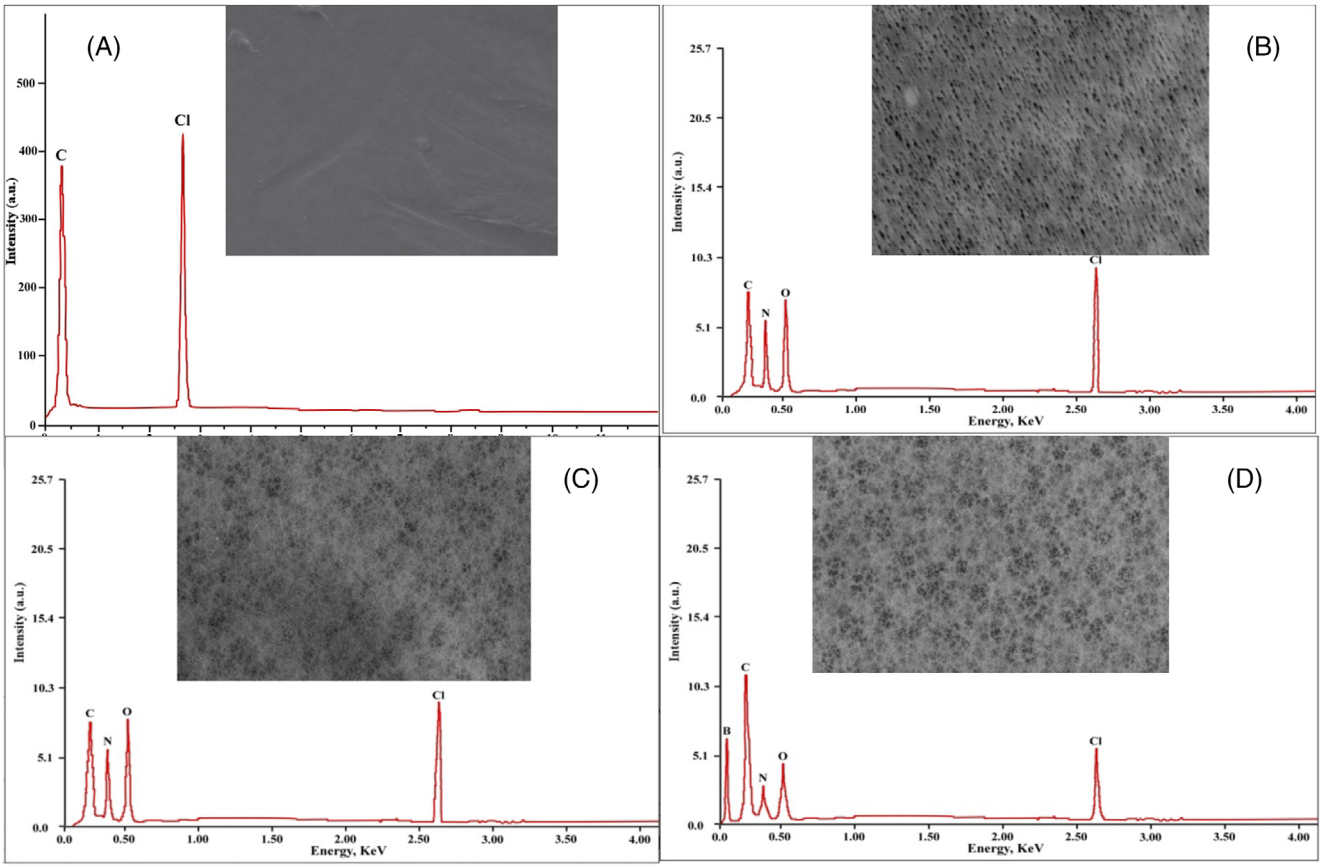

FIGURE 3 SEM–EDX of (A) PVC, (B) PVC-MG, (C) PVC-MG-NMDG, (D) PVC-MG-NMDG-B.

FIGURE 4 Thermogram of PVC, PVC-MG, PVC-MG-NMDG, and PVC-MG-NMDG-B in nitrogen atmosphere.

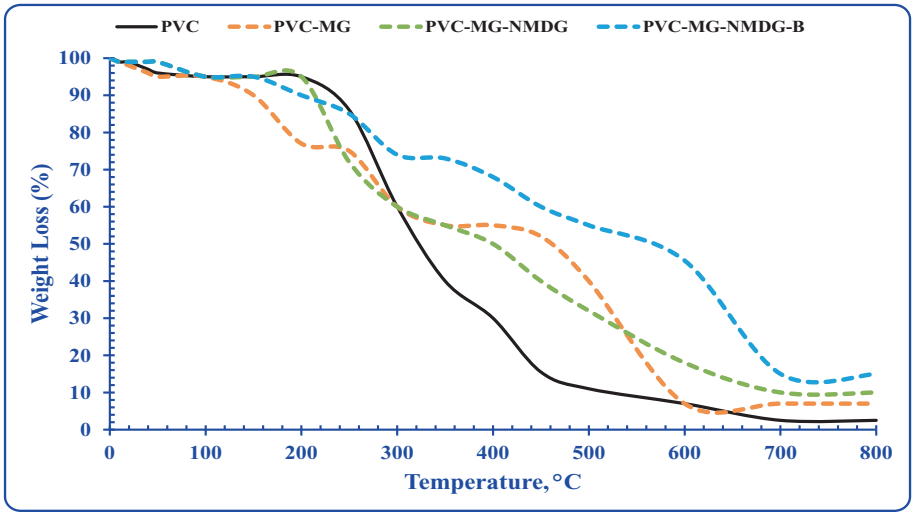

extraction of boron ions onto the PVC-MG-NMDG matrix, which raises the thermal property.[58]

3.2.6 | ^{1}H-NMR analysis

^{1}H-NMR investigation with the energy of 400 MHz, DMSO-d_6 as a diluent, and tetra methyl silane as a certified sample at 25°C is an effective device that stretches substantial data about protons in the manufactured PVC-MG-NMDG composite, which is estimated in the structure calculation. The chief δ (ppm) assignments for the unmodified PVC main skeleton appeared at 1.83 and 4.06, which were related to the $-(CH_2)_n$ and –CH–Cl groups, respectively. It was determined that the chemical shift value increases because the methine proton connected to the chlorine atom (an electronegative atom) is more de-shielded than the proton in a typical methylene

TABLE 3 TGA impacts of PVC, PVC-MG, PVC-MG-NMDG, and PVC-MG-NMDG-B.

Samples	PVC		PVC-MG		PVC-MG-NMDG		PVC-MG-NMDG-B	
TGA stages	Temp., °C	wt loss, %	Temp., °C	wt loss, %	Temp., °C	wt loss, %	Temp., °C	wt loss, %
1st	0–102	5	0–102	5	0–102	5	0–102	5
2nd	102–265	9	102–210	18	102–235	23	102–297	21
3rd	265–465	70.5	210–460	25	235–510	40	297–575	28.5
4th	450–600	13	460–600	45	510–600	22	575–600	30.5
Final residue	600–800	2.5	600–800	7	600–800	10	600–800	15

group. The other main δ (ppm) assignments for the branched PVC modified with methyl glycinate and N-methyl-D-glucamine appeared at 2.88, 3.87, 3.49, 2.89, 3.83, 6.27, and 4.76 ppm, which were related to methine group attached to nitrogen (–CH–N), nitrogen proton (–NH), methylene protons ($–CH_2$), methyl protons attached to nitrogen (CH_3–N–), methine proton attached to hydroxyl group (–OH), near the nitrogen atom, and finally hydroxy proton attached to methylene group ($–CH_2$–OH). The specification of the PVC-MG-NMDG composite using ^{1}H-NMR is demonstrated in Figure 5.

3.2.7 | ^{13}C-NMR analysis

^{13}C-NMR scrutiny with an energy of 100 MHZ and DMSO-d_6 as a diluent is a supportive device that stretches substantial data about the quantity of carbon atoms in the manufactured PVC-MG-NMDG composite. The main skeleton of the remaining unmodified PVC has the main δ (ppm) appearing at 57.5 and 39.7 ppm as singlets related to –CH–Cl carbon and methylene group $(–CH_2)_n$. The high value of the chemical shift of –CH–Cl carbon may be due to the attachment of the more electronegative chlorine atom. The main δ (ppm) assignments for the branched PVC appeared at 29.7, 45.3, 47.7, 50.7, 64.2, 72.2, and 170 ppm, which were related to branched $–CH_3$–N, (–CH–N), $–CH_2$, $–CH_2$OH, –CHOH, and –C=O carbons. The specification of the PVC-MG-NMDG composite using 13C-NMR is shown in Figure 6.

3.2.8 | Mass analysis

A mass spectrometer/gas chromatography unit (GC–MS) is utilized for the estimation of clarity, base peak (related to the further stable portion), and quasi-molecular ion peak (correlated to the molecular formulation). The quasi-molecular ion peak, which has a 264 value with a qualified abundance of 13%, embodies the molecular weight (M_w) of the manufactured PVC-MG-NMDG composite. Some significant fragmentation patterns, which are related to the manufactured PVC-MG-NMDG composite, were observed, such as $[C_2H_3Cl]_n^{\cdot}$ with m/z = 62 ($n = 1$), and a relative abundance of 15%, $[C_2H_5N]_n^{\cdot}$ with m/z = 43 ($n = 1$) and a relative abundance of 8%, $[C_2H_4N]_n^{\cdot}$ with m/z = 41 ($n = 1$) and a relative abundance of 11%. These observations assure the occurrence of remaining vinyl chloride building units in the chain of PVC-MG-NMDG composite. Additionally, other fragments were detected which reflected signs of the effective formation of PVC-MG-NMDG, such as $[C_6H_{15}NO_5]^{\cdot}$ with m/z = 181 and a relative abundance of 66%, which is related to N-methyl-D-glucamine, and $[CH_4O]^{\cdot}$ with m/z = 32 and a relative abundance of 47%, which is related to methyl alcohol. Alkyl and hydroxy radicals, which are caused by the fragmentation of the branched chain of the N-methyl-D-glucamine moiety, were observed, such as $[CH_3]$ with m/z = 15 and a relative abundance of 23% and $[OH]^{\cdot}$with m/z = 17 and a relative abundance of 12%.

It is public information that when PVC-MG-NMDG is exposed to an electron flux, HCl m/z = 36 with a relative abundance of 21% and $[H_2O]^{\cdot}$with m/z = 18 and a relative abundance of 55%) form the polymerized polyene, which can procedure cyclic compounds such as benzene $[C_6H_6]^{\cdot}$ with m/z = 78 and a relative abundance of 74%, ethyl benzene $[C_8H_{10}]^{\cdot}$ with m/z = 106 and a relative abundance of 90%, toluene $[C_7H_8]^{\cdot}$ with m/z = 92 and a relative abundance of 95%), and naphthalene $[C_{10}H_8]^{\cdot}$ with m/z = 128 and a relative abundance of 30%. The whole examination promises good preparation for the PVC-MG-NMDG composite. The description of PVC-MG-NMDG using GC–MS is exemplified in Figure 7.

3.3 | Profiles of extraction

3.3.1 | pH effect

Because pH marks the aquatic chemistry of boron and the active site appearances of the PVC-MG-NMDG

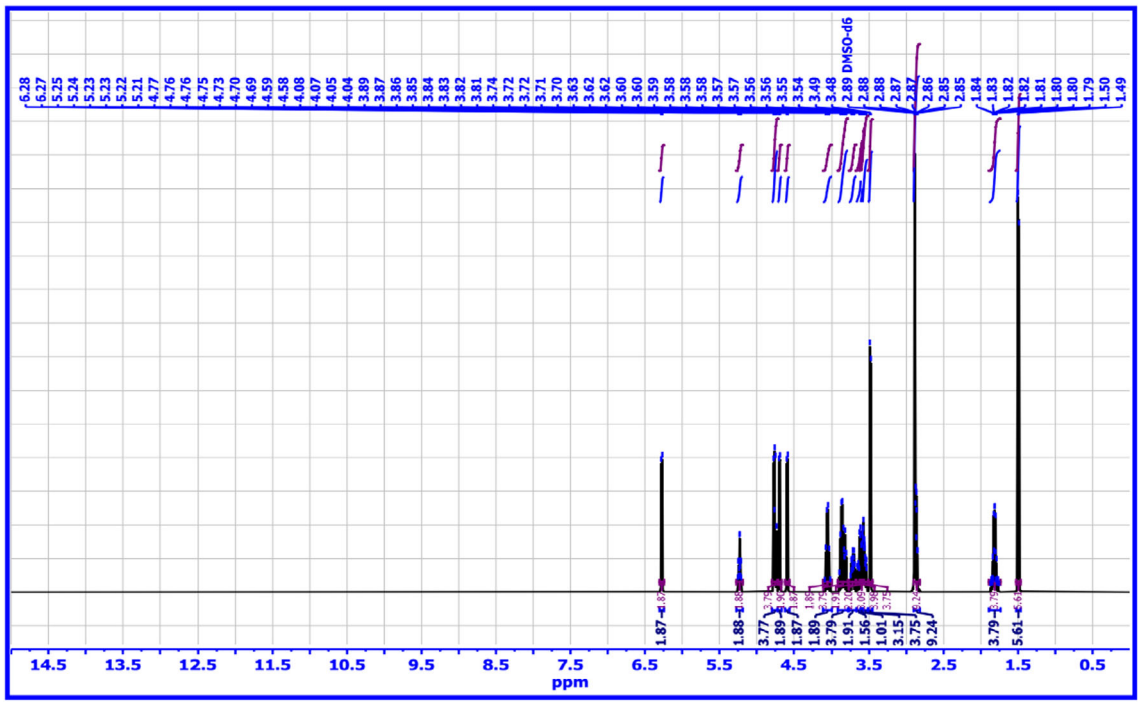

FIGURE 5 Specification of PVC-MG-NMDG composite by ^{1}H-NMR spectrometry.

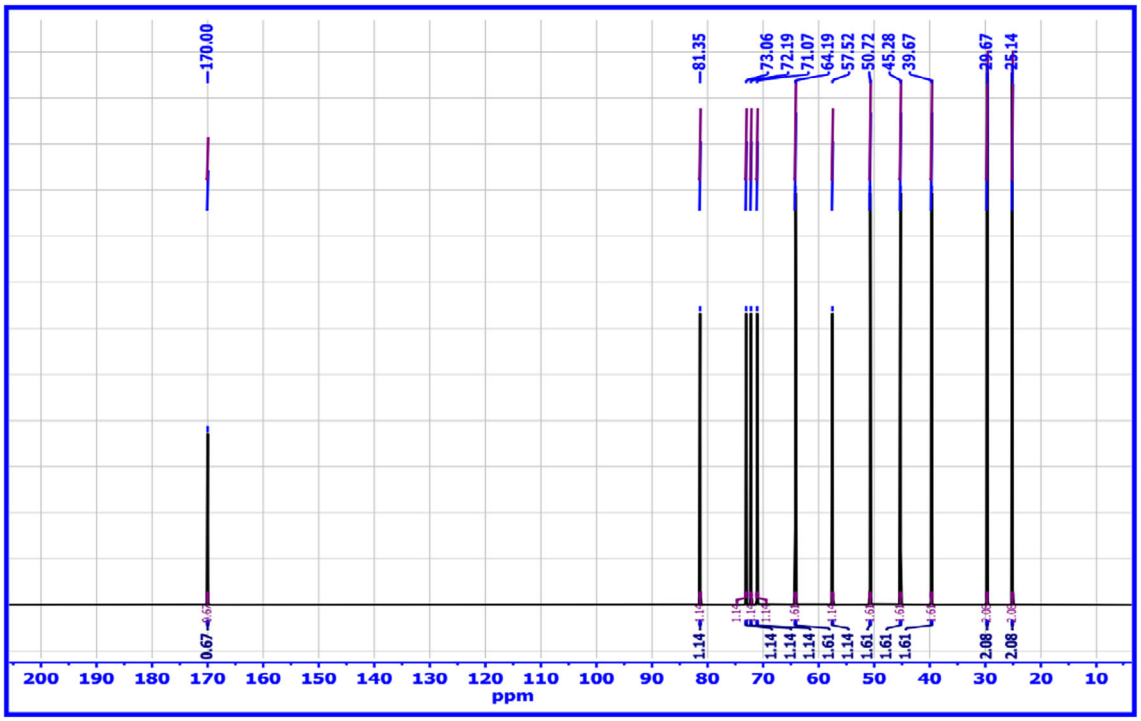

FIGURE 6 Specification of PVC-MG-NMDG composite by ^{13}C-NMR spectrometry.

composite, pH is critical to the retention of boron ions in the PVC-MG-NMDG composite. Figure 8 exemplifies the HYDRA-MEDUSA program's boron ion speciation at several pH values. Boron's solution chemistry is crucial because, depending on the solution's pH and boron content, boron can exist as either boric acid or a variety of other borates. Based on Equation (4), boric acid is a weak Lewis acid, with a pKa of 9.2 at 25°C.[59]

$$B(OH)_3 + OH^- \rightarrow B(OH)_4^-. \quad (4)$$

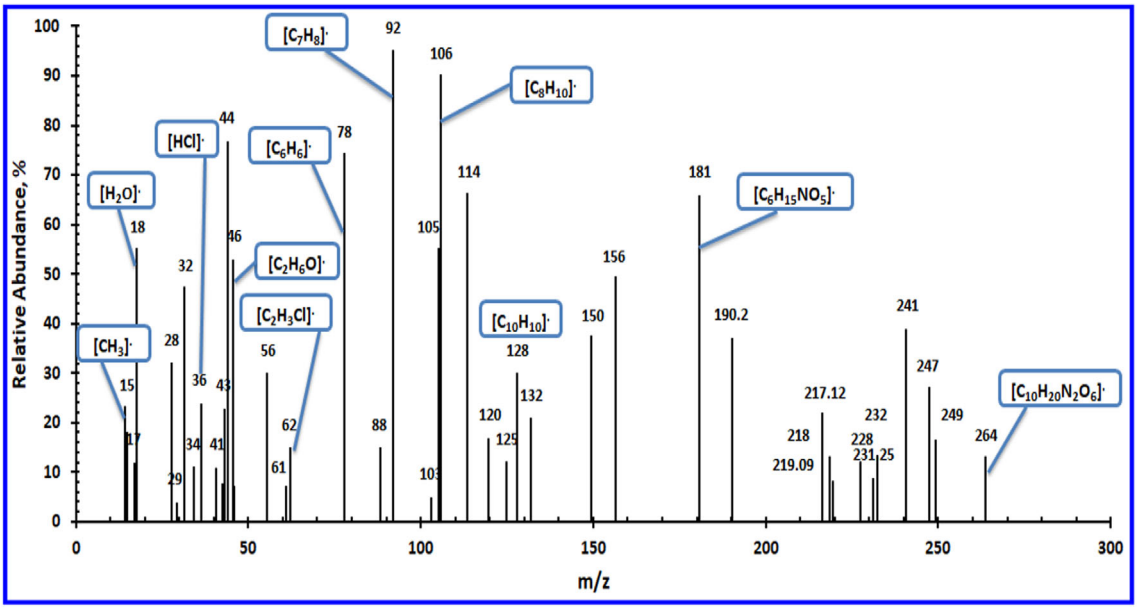

FIGURE 7 Specification of PVC-MG-NMDG composite by mass spectrometry.

Figure 8 shows that at low pH, boric acid predominates, while at high pH, borate ions predominate. There is also a minor concentration of $B(OH)_3$ and $B(OH)^{4-}$ (<216 mg/L) in the environment. Boron classes, namely $B_2O(OH)_6^{2-}$, $B_4O_5(OH)_4^{2-}$, $B_3O_3(OH)^{4-}$, and $B_5O_6(OH)^{4-}$ can be found in boron solutions at concentrations greater than 290 mg/L.[60,61]

The retention of boron ions on PVC-MG-NMDG composite was inspected at room temperature with 5 min of shaking via 25 mL of 150 mg/L boron ions (0.0138 mol/L) solution and 0.1 g of PVC-MG-NMDG composite at a pH range of 7–10. Figure 9A depicts the attained data, which reveals enhancement of the uptake capacity (q_{max}, mg/g) from pH 7 ($q_{max} = 0.75$ mg/g) to pH 9 ($q_{max} = 20$ mg/g) and remains constant till pH 10. The maximum adsorption capacity of boron ions at pH 9 ($q_{max} = 20$ mg/g) was detected since the anionic borate species predominate in this range. Consequently, a suggested pH of 9 is the ideal pH for boron ions retention on PVC-MG-NMDG composite, with an adsorption capability of $q_{max} = 20$ mg/g (80 ppm, 80%).

Straight line with a slope of 1.0632 and an intersection at 9.0472 is obtained from a linear regression study (slope analysis) involving a plot of log D versus pH (Figure 9B). Since 1 mole of hydrogen ion is released into a solution for every mole of boron chelated, the slope value defines the amount of hydrogen ions released through the formation of the PVC-MG-NMDG-B complex. Boric acid esters of borate anion complexes or boron containing a proton as a counter ion are common bonding mechanisms among polyoxide compound molecules. From the data, it appears that the occurrence of the

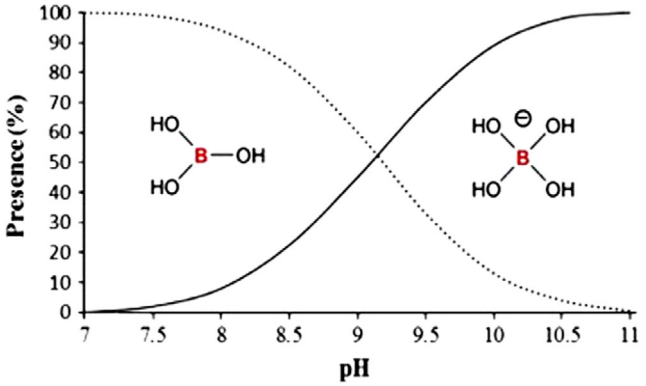

FIGURE 8 Boric acid and borate ion speciation-distribution as a function of solution pH.

amine group type in a tertiary is essential for chelating boron. It works by recapturing the proton released when hydroxyl functionalities complex borate.[11] The stability constant (β) of the PVC-MG-NMDG-B complex was mathematically considered at pH 9 (log β = 9.0472), which reflects a high affinity of the PVC-MG-NMDG composite towards boron ions.

3.3.2 | Impact of time of agitation

Agitation time is the most important variable. The impact of agitation time on boron ions capture from 2 to 30 min is examined by 0.1 g of PVC-MG-NMDG composite and 25 mL of 0.0138 mol/L boron aqueous solution (150 mg/L) at pH 9. The data are displayed in Figure 10A, which shows

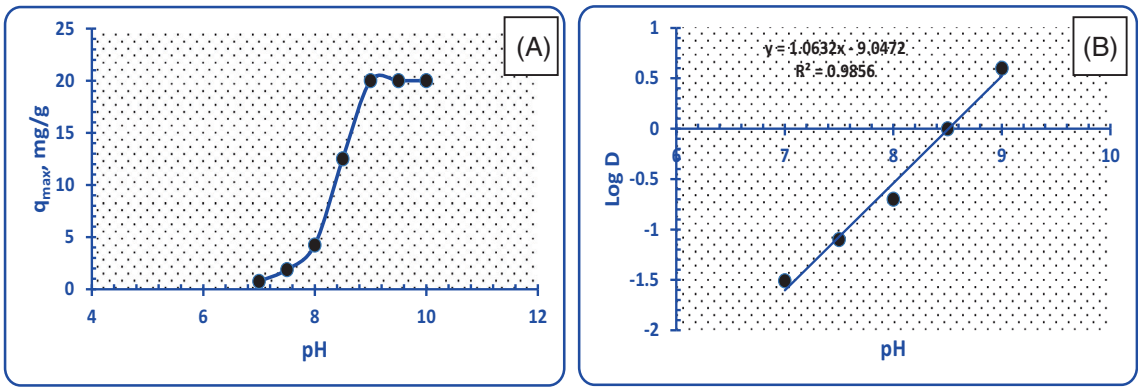

FIGURE 9 (A) The pH effect on boron retention by PVC-MG-NMDG composite (B) The slope regression study diagram for boron ions retention by PVC-MG-NMDG at diverse pH. (Conditions: V: 25 mL, B conc.: 150 mg/L, *m*: 0.1 g, *T*: 25°C, agitation time: 5 min).

that the maximum amount of boron ions adsorbed improves with an increasing period of agitation time and attains a maximum calculation value at 10 min (25 mg/g, 99% effectiveness), then remains nearly constant until 60 min. Consequently, 10 min were viewed as more than acceptable for equilibrium in succeeding experiments and were implemented in all succeeding studies, indicating good kinetics.

Kinetic prospects

The kinetics of boron ions adsorbed upon PVC-MG-NMDG composite designates the extraction rate. The extraction rate predictions can be calculated using kinetic parameters, which also give essential information for designing and modeling extraction procedures. Pseudo-first order, second order, and intra-particulate diffusion models were utilized to determine the extraction rate constants and the proposed mechanism for boron ions extraction on PVC-MG-NMDG composite. The next numerical equation describes the pseudo-first-order kinetic model.[62]

$$\mathrm{Log}(q_e - q_t) = \mathrm{Log}q_e - \left(\frac{K_1}{2.303}\right)t. \quad (5)$$

q_e is the equilibrium extraction rate of boron ions per mass unit, where K_1 (min^{-1}) denotes a constant rate. Figure 10B shows a straight line, the slope and intercept of which give the first order extraction rate constant K_1 and q_e values (q_e–q_t). The data may not be acceptable using pseudo-first order modeling, as depicted in the plot diagram below. The computed values of q_e were 28 mg/g, which is near the realistic value of 25 mg/g, at an extraction rate of $K_1 = 0.441\ \mathrm{min}.^{-1}$ and $R^2 = 0.9461$, but with a low correlation coefficient. The following equation defines pseudo-second order kinetic modeling[63]:

$$\frac{t}{q_t} = \frac{1}{k_2 {q_e}^2} + \left(\frac{1}{q_e}\right)t. \quad (6)$$

The constant k_2 denotes the rate (in grams per milligram per minute). The t/q_t line has a slope of $1/q_e$ and an intercept of $1/k_2{q_e}^2$. Figure 10C shows that pseudo-second-order kinetic modeling can be employed for the applied data. The premeditated mathematical value of q_e was 27.93 mg/g, nearly similar to the truthful investigational uptake of 25 mg/g, with a correlation coefficient $R^2 = 0.9903$ and extraction rate ($K_2 = 0.025$ g/mg min). The findings confirmed the second-order kinetic model is suitable for explaining the scheme under study, as it is consistent with the outcomes of the experiment. In light of the findings, second-order kinetic modeling is appropriate for the interpretation of the extraction system since it more closely resembles the experimental data.

The interaction between PVC-MG-NMDG and boron ions should be seen as a liquid–solid one. Several mechanisms exist for modulating boron ion extraction rates at the liquid–solid interface: (1) the diffusion of boron ions between spheres is observed in the second scenario (external diffusion mechanism); (2) intra-particle diffusion is a type of diffusion that takes place inside a particle (pore diffusion); and (3) the diffusion of boron ions from the bulk of the employed solution to the film around the composite-active site (bulk diffusion mechanism).[64]

Diffusion from outside the system controlled how fast the system was agitating, affecting how quickly the extract was extracted. The outer boundary or boundary layer thins as the agitation speed rises. Weber and Morris's intra-particle diffusion model equation is used to show boron ions extraction at various intervals, with the goal of identifying the square root of balancing time as a potential proportion determining stage of extraction of boron ions on the PVC-MG-NMDG composite.[65]

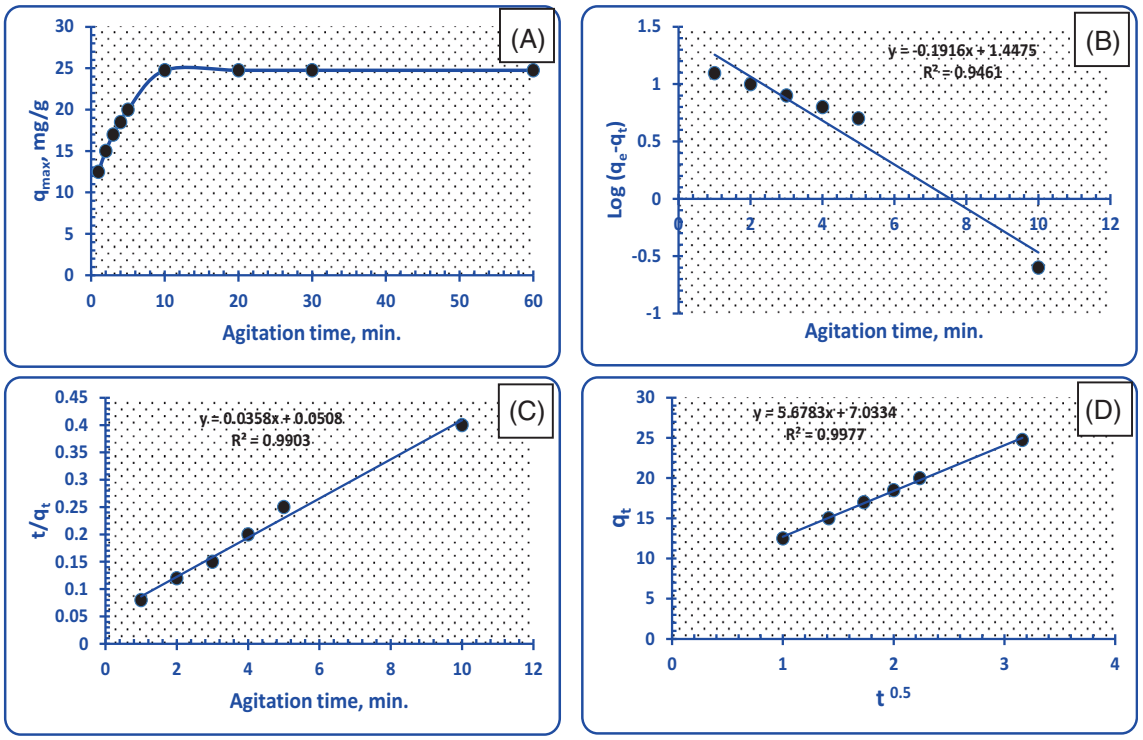

FIGURE 10 (A) Agitation time effect on boron ions uptake by PVC-MG-NMDG composite (B) first order (C) second order (D) intra-particle diffusion modelings. (Conditions: *V*: 25 mL, B conc.: 150 mg/L, *m*: 0.1 g, *T*: 25°C, pH: 9).

$$q_t = K_{ad}\sqrt{t} + I. \quad (7)$$

When q_t is the uptake of boron ions at t, K_{ad} denotes the proportion constant (mg/g $min^{-1/2}$), and I represents the thickness of the borderline layer. The pitch of the q_t linear inclinations against $t^{1/2}$ is exploited to compute the proportion constant (Figure 10D). The R^2 coefficient was beginning to be 0.9977, although the constant intra-particle diffusion proportion K_{ad} was 5.6783 mg/g $min^{-1/2}$ and the computed boundary layer thickness (I) was 7.0334. The positive value of (I) proposes that the mechanism of intra-particle diffusion could control boron ions extraction from PVC-MG-NMDG composites.

3.3.3 | Impact of initial boron ions concentration

Exploring the influence of initial concentration on boron ion uptake is crucial for determining the prospective uptake power. Boron ions uptake versus starting boron ion concentration in the two stages in Supplementary Figure 1a. Since saturating the PVC-MG-NMDG composite with boron ions at low boron concentrations was impossible, the boron uptake was significantly improved from 20 to 100 mg/L in the first step. The reason is that the PVC-MG-NMDG composite has more active sites than boron ions. Since the active sites in PVC-MG-NMDG have been saturated, the uptake of boron ions remains stable in the second step, from 100 to 200 mg/L. Hence, The maximum rate of boron uptake attained was 25 mg/g.

Distribution isotherm modeling

The total amount of boron ions removed to the PVC-MG-NMDG composite was determined at equilibrium and ambient temperature. For the Langmuir approach to work, it is necessary to assume that (a) the adsorbate molecules form a monolayer on the adsorbent surface, (b) the adsorption energy is constant, and (c) there is no adsorbate trans-migration on the surface plane. The derived equation describes the Langmuir isotherm model[66,67]:

$$\frac{C_e}{q_e} = \frac{1}{q_e b} + \frac{C_e}{q_e} \quad (8)$$

where C_e is the equilibrium concentration in milligrams per liter, q_e is the total amount of boron ions extracted at equilibrium, and q_e and b are Langmuir constants corresponding to the maximum extraction potential in milligrams per gram and the extraction energy in liters per milligram. To illustrate that the extraction mechanism is consistent with the Langmuir model,

Supplementary Figure 1b presents a linear plot of C_e/q_e versus C_e. $R^2 = 0.9995$ was found to be the correlation coefficient value for the linear regression model best fitting the Langmuir plot. Both q_e and b were computed using the slope and interception and were found to be 25.38 mg/g and 395.25 g/mg, respectively. To a greater extent than the experimental value (25 mg/g), the computed q_e agrees with the theoretical value. The fundamental characteristics of the Langmuir isotherm can be understood in terms of a dimensionless separation factor, or equilibrium parameter, RL, specified by the derived equation[68]:

$$R_L = \frac{1}{1 + bC_o}. \quad (9)$$

The concentration of boron ions at the outset was between 20 and 200 mg/L, and C_o represented this concentration in the expression, where b is the Langmuir constant. Good extraction of boron ions onto the PVC-MG-NMDG composite was reported to occur with R_L values between 0.00012 and 0.000012.

In addition, the Freundlich isotherm model was applied during extraction.[69,70] While purely mathematical, this formula is frequently employed in interpreting empirical findings. The equation represents the model of the Freundlich isotherm:

$$\mathrm{Log}q_e = \mathrm{Log}K_f + \left(\frac{1}{n}\right)\mathrm{Log}C_e. \quad (10)$$

In this equation, C_e represents the equilibrium concentration in milligrams per liter, q_e represents the total amount of boron ions extracted at equilibrium, and K_f and n indicate the extraction uptake capacity in milligrams per gram extraction rate, respectively. The constants K_f and n were calculated to be 16 mg/g and 2.335, respectively, using a linear plot of Log q_e against Log C_e. When (n) is between 0 and 10, it has also been demonstrated to extract useful information. The K_f value (16 mg/g) is less than the experimental value, and the $R^2 = 0.9319$ correlation coefficient between the two plots supports this. This indicates that Langmuir provides a better fit for the experimental results than Freundlich does Supplementary Figure 1c.

3.3.4 | The effect of the PVC-MG-NMDG composite dose

Boron ion absorption is predicted to be high because of its proximity to the sorbent-sorbate equilibrium in the process of extraction. Studying the influence of PVC-MG-NMDG composite doses from 0.025 to 0.5 g on boron ions extraction at constant boron concentration (150 mg/L), which is similar to the experimental supreme absorption capacity (25 mg/g), 0.1 g of PVC-MG-NMDG composite was used. Boron ion uptake increases from 0.025 to 0.1 g of PVC-MG-NMDG composite, as seen in Supplementary Figure 1d, before it begins to decrease when the number of active PVC-MG-NMDG composite sites is exhausted. In order to reduce the uptake of boron ions, increasing the PVC-MG-NMDG composite dose to a range between 0.2 and 0.5 g is necessary. This is because there are now more active sites in the PVC-MG-NMDG composite than there are boron ions. According to the data, a concentration of 0.1 g of PVC-MG-NMDG composite with an almost consumption uptake of 25 mg/g, could be a matched.

3.3.5 | Thermodynamic prospects

Extraction equilibrium and spontaneous extraction at different temperatures can be described using the significant thermodynamic parameters determined by Vant-Hoff and Gibb's free energy calculations. Contacting 0.1 g of PVC-MG-NMDG composite with 25 mL of aqueous boron solution with a concentration of 150 mg/L at pH 9 for 10 min at temperatures extending from 298 to 338 K, we can determine the influence of temperature upon boron ions uptake. It was explained that the adsorption capacity drops from 25 to 14.25 mg/g as the temperature rises from 298 to 338 K. Supplementary Figure 2a. shows that the extraction of boron ions onto the PVC-MG-NMDG composite increases in energy as the temperature rises, signifying that this process is exothermic.

In thermodynamics, this means determining changes in Gibbs free energy (ΔG, kJ/mol), enthalpy (ΔH, kJ/mol), and entropy (ΔS, J/mol K). The next equations were used to determine these thermodynamic characteristics[71]:

$$\Delta G = \Delta H - T\Delta S. \quad (11)$$

$$\mathrm{Log}K_d = \frac{\Delta S}{2.303R} - \frac{\Delta H}{2.303RT}. \quad (12)$$

To which the universal gas constant, R (8.314 J mol^{-1} K^{-1}), and the temperature, T (in Kelvin), are inputs (K). From the slope and intersection of the Log K_d against the $1/T$ plot (shown in Supplementary Figure 2b), we can derive the values of ΔH and ΔS, respectively, 717.7 and −2.116 (with an R^2 of 0.991).

As shown in Table 4, the extraction of boron ions from the PVC-MG-NMDG composite is an exothermic

process, as seen by the negative value of ΔH (−13.74 kJ/mol). The small negative value of ΔS (−0.04 kJ/mol) indicates a slight decrease in randomness during the extraction. The uptaking mechanism was shown to be thermodynamically spontaneous and achievable at low temperatures, as indicated by the negative ΔG values. Extraction is considered preferable at low temperatures, as the value of ΔG rises from (−1.82 kJ/mol at 298 K), (−1.42 kJ/mol at 308 K), (−1.02 kJ/mol at 3018 K), (−0.62 kJ/mol at 328 K), and (−0.19 kJ/mol at 338 K) as the temperature rises. The apparent activation energy (E_a) of boron ions extraction upon PVC-MG-NMDG composite at different temperatures may be calculated using the straight-line slope shown in Supplementary Figure 2b, which is why the Arrhenius equation is so valuable. Here is an equation that can be used to determine Arrhenius's equation[72]:

$$\mathrm{Log}K_d = \frac{-2.303E_a}{RT} + \mathrm{Log}A. \quad (13)$$

In this expression, K_d is the partition coefficient, E_a is the activation energy required for extraction in kilojoules per mole, R is the molar gas constant in degrees Kelvin (8.314 J/mol K), T is the temperature in kelvin, and A is the pre-exponential factor that is the temperature constant. The activation energy for extracting boron ions is −2.59 kJ/mol, as shown in a recent scientific study. Boron ion extraction upon a PVC-MG-NMDG composite is an exothermic process that occurs spontaneously at ambient temperature without activation energy, making the extraction process less sensitive to temperature.

3.3.6 | The effect of co-ions

Since most co-ions are removed during the alkali fusion process employed for boron mineral opening as insoluble hydroxides, the analyzed potential co-ions are identified as co-ions with boron in the leach liquor. Sodium borate, however, remained soluble in the leach liquor. This means that most co-ions may be present in the leach liquor at a low concentration. Co-existing ions' effects were investigated by adding them one at a time to a 150 mg/L boron solution in water, pH 9, and mixing it with 0.1 g of PVC-MG-NMDG composite at 25°C for 10 min to determine the optimal extraction conditions. The efficiency and selectivity of PVC-MG-NMDG composites towards boron ions are governed by the separation factor parameter, represented by (S.F).

Table 5 shows that the PVC-MG-NMDG composite successfully extracted boron ions in the later optimal circumstances, with a separation factor that met or exceeded expectations. It was found that metal cations such as Na^+, K^+, Si^{4+}, Al^{3+}, Ca^{2+}, and Mg^{2+} could be used to obtain a high S.F., but that heavy metals such as Fe^{3+}, Fe^{3+}, Cr^{3+}, Mn^{2+}, Ni^{2+}, Zn^{2+}, and V^{5+} could have a minor impact on boron ion extraction and be co-extracted at the same time with boron ions with varying separation. An important notice should be mentioned as PVC-MG-NMDG composite has an excessive ability to

TABLE 4 The thermodynamic indices of boron ions extraction upon PVC-MG-NMDG composite.

Parameter	ΔH, kJ/mol	ΔS, kJ/mol K	ΔG, kJ/mol				
B^{3+}	−13.74	−0.04	298 K	308 K	318 K	328 K	338 K
			−1.82	−1.42	−1.02	−0.62	−0.19

TABLE 5 The co-ions effect upon boron extraction upon PVC-MG-NMDG composite.

Co-ions	Feed soln. mg/L	Raffinate, mg/L	S.F[a]	Co-ions	Feed soln. mg/L	Raffinate, mg/L	S.F[a]
B^{3+}	150	50	—	Fe^{3+}	1000	900	891.89
Na^+	1000	1000	99×10^3	Ti^{4+}	1000	930	1320
K^+	1000	1000	99×10^3	Ca^{2+}	1000	970	3300
Si^{4+}	1000	1000	99×10^3	Mg^{2+}	1000	950	1903
Al^{3+}	1000	1000	99×10^3	V^{5+}	1000	730	267.56
Mn^{2+}	1000	950	1903	Cr^{3+}	1000	810	423.07
Fe^{2+}	1000	980	4950	Zn^{2+}	1000	960	2414.63
Pb^{2+}	1000	910	1010.2	Ni^{2+}	1000	955	2106.38

Note: Conditions: V: 25 mL, boron conc.: 150 mg/L, m: 0.1 g, T: 25°C, agitation time: 10 min, pH 9.

[a]Separation factor (S.F): The partition coefficient of boron ions (D_B) over the partition coefficient of co-ions (D_M).

bind boron ions, which establishes that raising the separation impact will enable the separation of the co-ions from boron ions by multi-stage extraction.

3.3.7 | Boron back extraction and precipitation

At ambient temperature, utilizing acid of 15 mL volume for 0.1 g of loaded PVC-MG-NMDG composite within 5 min of agitation, three different eluting agents (H_2SO_4, HCl, and HNO_3) with different concentrations from 0.025 to 1 M were tested as eluting agents for the elution of boron ions from the loaded PVC-MG-NMDG composite. It was discovered, based on the data that were obtained and displayed in Table 6, that the boron ions back extraction efficiency improves at high concentrations, but completely disappears when the concentration is decreased. With 0.5 M H_2SO_4, it was feasible to achieve an elution efficiency of 95%; with 1 M HCl, it was possible to achieve 96%; and with 0.5 M HNO_3, it was possible to achieve 99%. For economic aspects, 0.5 M H_2SO_4 (95% elution efficiency) is used to elute boron ions from the loaded PVC-MG-NMDG composite. The solution of elution is exposed to vaporization to prepare a concentrate of boric acid from the eluted solution, where boric acid is crystallized as a final product.[73]

TABLE 6 Eluting agents conc. impact upon boron ions elution from boron-loaded PVC-MG-NMDG composite.

	Elution efficiency, (%)		
Acid conc., (M)	**H_2SO_4**	**HCl**	**HNO_3**
0.025	88.6	91	93
0.05	90.5	92	95
0.1	93	94	97
0.5	95	93.5	99
1	95	96	99

3.3.8 | Mineralogical and chemical composition of a tourmaline ore sample

The mineralogical analysis of the Sikait tourmaline ore sample, Eastern Desert, Egypt, has confirmed the presence of two tourmaline mineral types, for example, Fe-type Schorl mineral ($NaFe_3Al_6B_3Si_6O_{27}$ $(OH)_4$) [ASTM cart No., 22-469],[74] and Mg-type Dravite mineral ($NaMg_3Al_6B_3Si_6O_{27}(OH)_4$), [ASTM cart No., 14-76].[75] On the other hand, the complete chemical scrutiny of the ore sample revealed the presence of major components such as B_2O_3 assays at 10.43%, SiO_2 assays at 35.45%, Al_2O_3 assays at 31.72%, FeO assays at 9.3%, and MgO assays 8.1%. In the meantime, some trace elements have been analyzed, as shown in Table 7.

3.3.9 | Dissolution of tourmaline ore sample

The Sikait tourmaline ore sample from the Eastern Desert of Egypt was treated with alkali fusion leaching technology, which involved the use of sodium hydroxide flux to free boron in the form of sodium borate, and then the ore was washed in hot water to extract any remaining metals. First, the tourmaline ore was crushed and then sieved to a size of 74 μm (−200 mesh). Two hours of fusing at 850°C with NaOH flux and an alkali/ore mass ratio of 2/1 of the stoichiometric amount of tourmaline ore resulted in optimal fusion. Once the alkali fusion process was complete and the product had cooled, it has been ground and sieved to a grain size of 74 μm before being leached in hot water for 30 min at a solids-to-liquids ratio of 1 g/100 mL. After further optimizing the leaching variables, it was shown that the effectiveness of boron

TABLE 7 Chemical conformation of Sikait tourmaline ore sample.

Component	Content (%)	Component	Content (mg/L)
B_2O_3	10.43	Mn	693
SiO_2	35.54	Zn	160
Al_2O_3	31.72	Ni	137
Fe_2O_3 total	9.3	Cr	136
CaO	0.28	V	203
MgO	8.1	Cu	35
Na_2O	2.3		
K_2O	0.03		
TiO_2	0.17		
Loss in ignition	1.5		

leaching using alkali fusion technology could reach 99%.[76,77] The alkali fusion technology by sodium hydroxide using an electrical oven at 850°C is totally differing from the ordinary leaching. The optimized fusion factors using sodium hydroxide can destruct effectively the crystal lattice of the Tourmaline mineral resulting in boron liberation as soluble borate, $B(OH)^{4-}$, which can be extracted by the composite, while the other co-ions precipitate as hydroxides. Hence, this step helps to get rid of the most co-ions associated with boron. It is crucial to remove the silica gel formed as a by-product from the prepared alkaline leach liquor as soon as possible after the hot water leaching process has been completed. The objective is to prevent silica gel from coating the

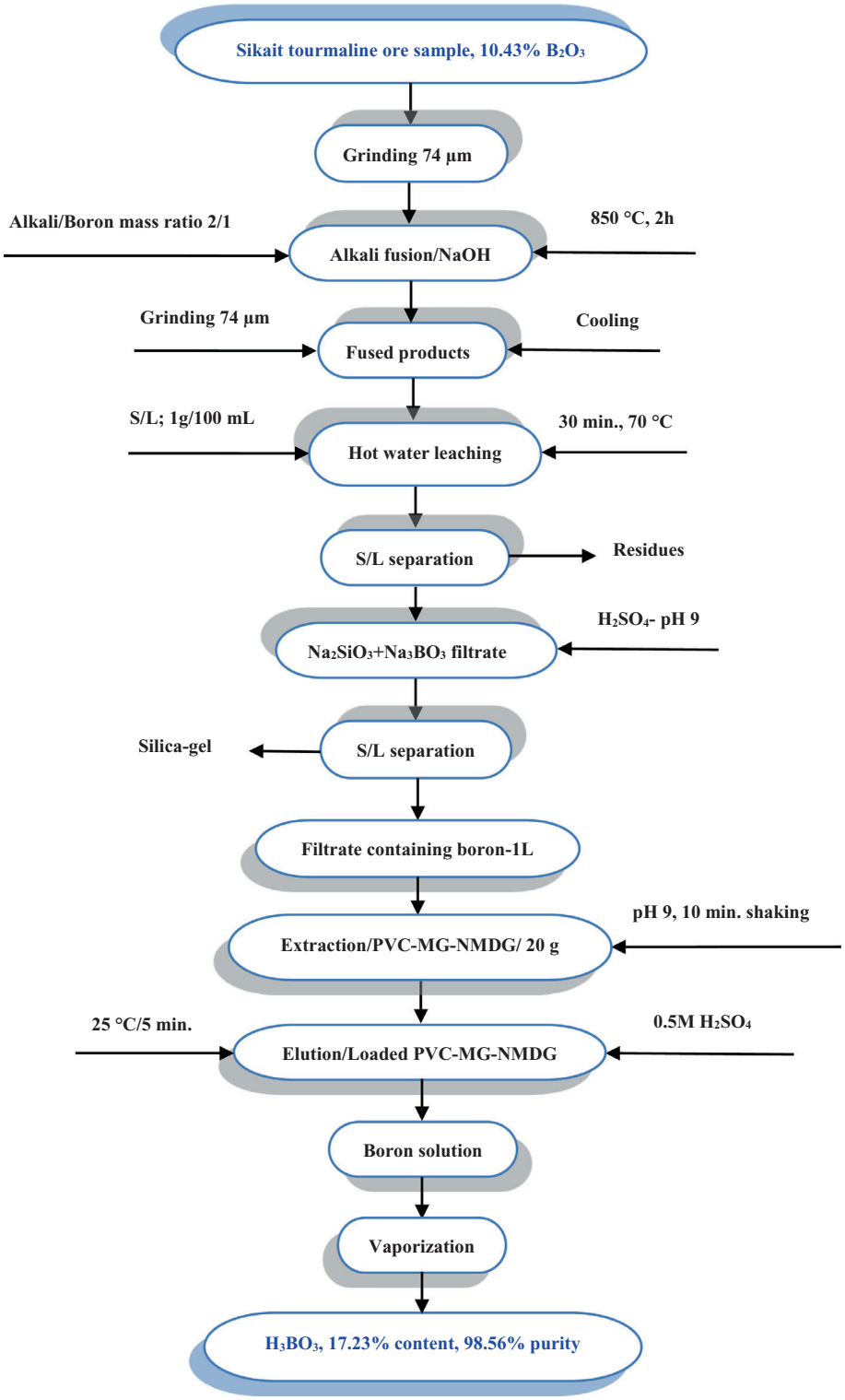

FIGURE 11 A flow chart with boron mass balance for preparing pure H_3BO_3 from Sikait tourmaline ore sample, Eastern Desert, Egypt, using PVC-MG-NMDG composite.

PVC-MG-NMDG composite, which would result in fouling of the composite. This was accomplished by adding concentrated hydrogen sulfide to the prepared alkali leach liquid to raise its pH level to 9. During the filtration process, the precipitated silica in the form of SiO_2-gel needs to be washed with dilute H_2SO_4 (1%) to prevent the loss of any dissolved boron that could occur due to adsorption on its outer surface. After that, the precipitate of SiO_2-gel was heated to 850°C for 2 h, after which it was allowed to cool and be cleaned. SiO_2 was obtained following the drying process.[78] After solid–liquid separation, the Raffinate containing boron could be selectively extracted onto the PVC-MG-NMDG composite.

3.3.10 | Application: Boron recovery from Sikait tourmaline ore sample, Eastern Desert, Egypt, by PVC-MG-NMDG composite

The optimized results make it possible to use PVC-MG-NMDG composites to extract boron at pH 9. The applied experiment was completed under the optimal conditions that had been determined in advance, which were as follows: pH = 9, agitation time = 10 min, and temperature = 25°C. This was accomplished by mixing 1 liter of leach liquor with 20 g of PVC-MG-NMDG composite. The extraction experiment was replicated until composite saturation, with a maximum uptake capability of 25 mg/g. According to the findings, the composite has a boron extraction effectiveness of up to 99%. This was determined by analyzing the data. Otherwise, it was also documented that the extracted boron upon the composite can be easily eluted by 250 mL of 0.5 M H_2SO_4 within 10 min to obtain boric acid.

The eluted boron solution is vaporized to attain highly pure boric acid with the lowest impurities. The product was redissolved in H_2O that had been distilled for further purification before being transferred to a PVC-MG-NMDG composite. The eluate-rich boron solution was re-crystallized by evaporation after the loading and elution operations were completed to create high-purity H_3BO_3 acid. ICP-OES, XRD, and FTIR analysis are utilized in characterizing boric acid concentrate to determine the amount of boron present and the metal ions that are linked with it. Supplementary Figure 4 and Figure 11, as well as Table 8, present the study's findings. Based on the findings, it is possible to conclude that the concentration of boric acid produced by the PVC-MG-NMDG composite has a boron content of 17.23% while maintaining a purity level of 98.56%. Epitomizes a representation flow chart that explicates the boron recovery from the Sikait tourmaline ore sample in the Eastern Desert, Egypt.

TABLE 8 ICP-OES analysis of pure boric acid concentrate.

Element	Content, (%)	Element	Content, (%)
B	17.23	Mg	0.0034
Si	0.051	Ti	0.0031
Al	0.035	V	0.021
Na	0.0011	Cr	0.0037
K	0.0013	Mn	0.0045
Ca	0.0019	Zn	0.0055

TABLE 9 Different composites for boron extraction from different matrices.

Ligand	q_{max}, mg/g	References
Amberlite IRA-743	5–7	81
Polyol grafted SBA-15	6.3	82
NMDG-MCM-41	8	45
CCTs-NMDG	21	38
NMDG-type cellulose derivatives	11	83
Poly(styryl sulfonamide) resin	23.6	84
PAN-g-PG	34.59	83
P(GMA-co-TRIM)-MG	19.9	85
PVC-MG-NMDG composite	25	Present study

Supplementary Figure 3 presents the results of the XRD performed on the obtained boric acid crystal. The crystal structure of the boric acid product conformed to PDF Code No. 01-73-2158, which is related to the mineral Sassolite and has distinct 2θ angles at 14.52, 14.95, 28, and 40°. These angles can be found at the relevant spots where they are positioned. The triclinic phase of the Sassolite mineral was verified to be present thanks to the preferred orientation of boric acid along the (100) plane (H_3BO_3).[79] As can be observed, the diffraction peaks of boric acid were distinct, and there was no evidence of an impurity peak. This indicates that boric acid had a well-organized crystal structure and was of quite high purity. Through the use of FTIR spectroscopy, the functional groups that are found in boric acid were investigated, and the resulting spectrum can be seen in Supplementary Figure 4. The existence of a number of peaks demonstrated the vibrations produced by the different functional groups that were present in the sample. The stretching vibrations of the OH bond can be seen since there is a peak at 3205 cm^{-1} in the spectrum. The –CH stretching vibrations may be responsible for the peaks at 2358 and 2252 cm^{-1}. It is possible that the peak

at 1184 cm^{-1} is caused by the out-of-plane bending vibrations of -B-OH, while the peak at 1350 cm^{-1} is caused by the asymmetric stretching vibrations of -B-O. The vibrations of the atoms in the B-O bond are represented by the peak at 643 cm^{-1}, while the peak represents the bending vibrations of the O-B-O bond at 538 cm^{-1}.[80]

A comparative study of different chelating ligands for boron extraction from different matrices is shown in Table 9. The proposed flowsheet for boron extraction from a Sikait tourmaline ore sample from the Eastern Desert, Egypt, using PVC-MG-NMDG composite is presented in Figure 11.

4 | CONCLUSION

A productive synthesis of N-methyl-D-glucamine modified polyvinyl chloride via methyl glycinate linker (PVC-MG-NMDG) composite is applicable for boron ions extraction from a Sikait tourmaline ore sample in the Eastern Desert, Egypt. Numerous techniques, including FT-IR, XPS, BET, EDX, TGA, ^{1}H-NMR, ^{13}C-NMR, GC–MS, XRD, and ICP-OES, were utilized to complete the characterizations successfully. The static extraction method was perfected by using a sufficient volume of a solution of 25 milliliters with a concentration of 100 mg/L of boron ions, which was then mixed with 0.1 g of a PVC-MG-NMDG composite at a pH of 9 for 10 min at room temperature. The produced composite reached its maximum absorption of 25 mg/g at 25°C when these conditions were present. Taking into account economic factors, this was an ideal result. The linear regression analysis, which includes plotting log D against pH, results in a straight line with a slope of 1.0632. This proves that 1 mole of hydrogen ions is free in the solution, which protonates the nitrogen in the N-methyl-D-glucamine moiety. At a pH of 9, the value of the stability constant (β) of the PVC-MG-NMDG-B complex was estimated to be ($\log \beta = 9.0472$). The data obtained for the kinetic modeling was a good fit with the pseudo-second-order model, which provides a better explanation of the extraction process in question. This model predicts an uptake of 27.93 mg/g, close to the experimental result of 25 mg/g. The fact that I, the thickness of the boundary layer, had a positive value shows that the intra-particle diffusion mechanism would be responsible for regulating the extraction of boron ions from the PVC-MG-NMDG composite.

Modeling distribution isotherms, the Langmuir isotherm model is most adapted to follow the retention mechanism, resulting in an adsorption value of 25.38 mg/g. This is the more conventionally employed value. According to the calculated thermodynamic profiles, the spontaneous, anticipated, and exothermic advantageous extraction at low temperatures was realized. Also taken into account were the thermodynamic parameters controlling ΔS (−0.04 kJ/mol), ΔH (−13.74 kJ/mol), and ΔG. As the temperature increases from 298 to 338°C, the value of ΔG drops from −1.82 to −0.19 kJ/mol. With 0.5 M H_2SO_4, boron ions were 95% efficiently eluted from boron-loaded PVC-MG-NMDG. For the vast majority of co-ions, the PVC-MG-NMDG composite demonstrates a flawless separation factor (S.F.). Alkali fusion with NaOH flux, followed by extraction with PVC-MG-NMDG composite, produces a high-purity boric acid concentrate with a boron concentration of 17.23% and a purity of 98.56%.

ACKNOWLEDGMENT

The authors have received no financial and material support for this study.

CONFLICT OF INTEREST STATEMENT

The authors declare no conflicts of interest.

DATA AVAILABILITY STATEMENT

Data availability is not applicable.

ORCID

Huda M. Younis https://orcid.org/0000-0002-5680-8522
Amal A. Mohamed https://orcid.org/0000-0001-6364-299X

REFERENCES

1. Hilal N, Kim GJ, Somerfield C. Boron removal from saline water: a comprehensive review. *Desalination*. 2011;273:23-35. doi:10.1016/j.desal.2010.05.012
2. Bodzek M. The removal of boron from the aquatic environment-state of the art. *Desalin Water Treat*. 2016;57:1107-1131. doi:10.1080/19443994.2014.1002281
3. Wang B, Guo X, Bai P. Removal technology of boron dissolved in aqueous solutions – a review. *Colloids Surf A Physicochem Eng Asp*. 2014;444:338-344. doi:10.1016/j.colsurfa.2013.12.049
4. Parks JL, Edwards M. Boron in the environment. *Crit Rev Environ Sci Technol*. 2005;35(2):81-114. doi:10.1080/10643380590900200
5. Guan Z, Lv J, Bai P, Guo X. Boron removal from aqueous solutions by adsorption-a review. *Desalination*. 2016;383:29-37. doi:10.1016/j.desal.2015.12.026
6. Nasef MM, Nallappan M, Ujang Z. Polymer-based chelating adsorbents for the selective removal of boron from water and wastewater: a review. *React Funct Polym*. 2014;85:54-68. doi:10.1016/j.reactfunctpolym.2014.10.007
7. Kameda T, Oba J, Yoshioka T. Use of Mg-Al oxide for boron removal from an aqueous solution in rotation: kinetics and equilibrium studies. *J Environ Manage*. 2016;165:280-285. doi:10.1016/j.jenvman.2015.09.035
8. Terekhova AM, Levchenko YV, Matveeva TV, Borisov IS, Chelmakov IA. Influence of boron enrichment in control rods

on neutron-physical characteristics of the core of the reactor VVER. *IOP Conf Series Mater Sci Eng*. 2019;487:012007. doi:10.1088/1757-899X/487/1/012007

9. Novich KA, Pedersen SV, Borrelli R, Christensen R, Jaques BJ. Synthesis of boron carbide reinforced aluminum castings through mechanical stir casting. *J Compos Mater*. 2021;55:1-2177. doi:10.1177/0021998320987597
10. Singh VP, Badiger NM. γ-ray interaction characteristics for some boron containing materials. *Vacuum*. 2015;113:24-27. doi:10.1016/j.vacuum.2014.11.011
11. Wolsk J, Bryjak M. Methods for boron removal from aqueous solutions–a review. *Desalination*. 2013;310:18-24. doi:10.1016/j.desal.2012.08.003
12. Tu KL, Chivas AR, Nghiem LD. Effects of chemical preservation on flux and solute rejection by reverse osmosis membranes. *J Membr Sci*. 2014;472:202-209. doi:10.1016/j.memsci.2014.08.052
13. Ezechi EH, Isa MH, Kutty SRM, Yaqub A. Boron removal from produced water using electrocoagulation. *Process Saf Environ Prot*. 2014;92:509-514. doi:10.1016/j.psep.2014.08.003
14. Sari MA, Chellam S. Mechanisms of boron removal from hydraulic fracturing wastewater by aluminum electrocoagulation. *J Colloid Interface Sci*. 2015;458:103-111. doi:10.1016/j.jcis.2015.07.035
15. Dydo P, Turek M. Boron transport and removal using ion-exchange membranes: a critical review. *Desalination*. 2013;310:2-8. doi:10.1016/j.desal.2012.08.024
16. Kir E, Gurler B, Gulec A. Boron removal from aqueous solution by using plasmamodified and unmodified anion-exchange membranes. *Desalination*. 2011;267:114-117. doi:10.1016/j.desal.2010.08.037
17. Akretche DE, Kerdjoudj H. Donnan dialysis of copper, gold and silver cyanides with various anion exchange membranes. *Talanta*. 2000;51:281-289. doi:10.1016/s0039-9140(99)00261-1
18. Remy P, Muhr H, Plasari E, Ouerdiane I. Removal of boron from wastewater by precipitation of a sparingly soluble salt. *Environ Prog*. 2005;24:105-110. doi:10.1002/ep.10058
19. Yoshikawa E, Sasaki A, Endo M. Removal of boron from wastewater by the hydroxyapatite formation reaction using acceleration effect of ammonia. *J Hazard Mater*. 2012;237-238:277-282. doi:10.1016/j.jhazmat.2012.08.045
20. Samatya S, Köseoğlu P, Kabay N, Tuncel A, Yüksel M. Utilization of geothermal water as irrigation water after boron removal by monodisperse nanoporous polymers containing NMDG in sorption-ultrafiltration hybrid process. *Desalination*. 2015;364:62-67. doi:10.1016/j.desal.2015.02.030
21. Tagliabue M, Reverberi AP, Bagatin R. Boron removal from water: needs, challenges and perspectives. *J Clean Prod*. 2013;77:1-9. doi:10.1016/j.jclepro.2013.11.040
22. Peng X, Li L, Shi D, et al. Recovery of boric acid from salt lake brines by solvent extraction with 2-butyl-1-n-octanol. *Hydrometallurgy*. 2018;177:161-167. doi:10.1016/j.hydromet.2018.03.013
23. Abdallh M, Bufaroosha M, Ahmed A, Ahmed DS, Yousif E. Modification of poly(vinyl chloride) substrates via Schiff's base for photochemical applications. *J Vinyl Addit Technol*. 2020;26:475-480. doi:10.1002/vnl.21762
24. Balinski A, Recksiek V, Kelly N. Solvent extraction of boric acid: comparison of five different monohydric alcohols and equilibrium modeling with numerical methods. *Processes*. 2021;9:398. doi:10.3390/pr9020398
25. Guo J, Yang Y, Gao X, Yu J. Boron extraction from lithium-rich brine using mixed alcohols. *Hydrometallurgy*. 2020;197:105477. doi:10.1016/j.hydromet.2020.105477
26. Xu Z, Su H, Zhang J, et al. Recovery of boron from brines with high magnesium content by solvent extraction using aliphatic alcohol. *RSC Adv*. 2021;11:16096-16105. doi:10.1039/d1ra01906f
27. Brooks WLA, Deng CC, Sumerlin BS. Structure–reactivity relationships in boronic acid–diol complexation. *ACS Omega*. 2018;3(12):17863-17870. doi:10.1021/acsomega.8b02999
28. Zhang R, Xie Y, Song J, et al. Extraction of boron from salt lake brine using 2-ethylhexanol. *Hydrometallurgy*. 2016;160:129-136. doi:10.1016/j.hydromet.2016.01.001
29. Kwon T, Hirata M, Hano T, Yamagishi T. Equilibrium of boron extraction with 2-butyl-2-ethyl-1,3-propanediol and 2-ethylhexanol in butyl acetate. *Sep Sci Technol*. 2005;40(7):1415-1424. doi:10.1081/SS-200052840
30. Fan X, Yu X, Guo Y, Deng T. Recovery of boron from underground brine by continuous centrifugal extraction with 2-ethyl-1,3-hexanediol (EHD) and its mechanism. *J Chem*. 2018;2018:1-8. doi:10.1155/2018/7530837
31. Peng X, Shi D, Zhang Y, Zhang L, Ji L, Li L. Recovery of boron from un acidified salt lake brine by solvent extraction with 2,2,4-trimethyl-1,3-pentanediol. *J Mol Liq*. 2021;326:115301. doi:10.1016/j.molliq.2021.115301
32. Bonin L, Deduytsche D, Wolthers M, Flexer V, Rabaey K. Boron extraction using selective ion exchange resins enables effective magnesium recovery from lithium rich brines with minimal lithium loss. *Sep Purif Technol*. 2021;275:119177. doi:10.1016/j.seppur.2021.119177
33. Kabay N, Yilmaz I, Yamac S, et al. Removal and recovery of boron from geothermal wastewater by selective ion exchange resins. I. Laboratory tests. *React Funct Polym*. 2004;60:163.
34. Zhang N, Lyu J, Bai P, Guo X. Boron isotopic separation with pyrocatechol-modified resin by chromatography technology: experiment and numerical simulation. *J Indus Eng Chem*. 2018;57:244-253. doi:10.1016/j.jiec.2017.08.030
35. Li X, Liu R, Wu S, Liu J, Cai S, Chen D. Efficient removal of boron acid by N-methyl-D-glucamine functionalized silica-polyallylamine composites and its adsorption mechanism. *J Colloid Interface Sci*. 2011;361:232-237. doi:10.1016/j.jcis.2011.05.036
36. Senkal BF, Bicak N. Polymer supported iminodipropylene glycol functions for removal of boron. *React Funct Polym*. 2003;55:27-33. doi:10.1016/S1381-5148(02)00196-7
37. Sanchez J, Wolska J, Yorukoglu E, Bernabe L, Bryjak M, Kabay N. Removal of boron from water through soluble polymer based on N-methyl-D-glucamine and regenerated-cellulose membrane. *Desalin Water Tret*. 2016;57(2):861-869. doi:10.1080/19443994.2014.979369
38. Gaballah ST, Khalil AM, Rabie ST. Thiazole derivatives-functionalized polyvinyl chloride nanocomposites with photostability and antimicrobial properties. *J Vinyl Addit Technol*. 2019;25:E137-E146. doi:10.1002/vnl.21670
39. Thakur N, Kumar SA, Shinde RN, Pandey AK, Kumar SD, Reddy AVR. Extractive fixed-site polymer sorbent for selective boron removal from natural water. *J Hazard Mater*. 2013;260:1023-1031. doi:10.1016/j.jhazmat.2013.06.051

40. Bicak N, Senkal BF. Sorbitol-modified poly(N-glycidyl styrene sulfonamide) for removal of boron. *J Appl Polym Sci*. 1998;68:2113-2119.
41. Geffen N, Semiat R, Eisen MS, Balazs Y, Katz I, Dosoretz CG. Boron removal from water by complexation to polyol compounds. *J Membr Sci*. 2006;286:45-51. doi:10.1016/j.memsci.2006.09.019
42. Luo Q, Zeng M, Wang X, et al. Glycidol-functionalized macroporous polymer for boron removal from aqueous solution. *React Funct Polym*. 2020;150:104543. doi:10.1016/j.reactfunctpolym.2020.104543
43. Bicak N, Gazi M, Senkal BF. Polymer supported amino bis-(cis-propan2,3 diol) functions for removal of trace boron from water. *React Funct Polym*. 2005;65:143-148. doi:10.1016/j.reactfunctpolym.2005.01.010
44. Liu H, Ye X, Li Q, et al. Boron adsorption using a new boron-selective hybrid gel and the commercial resin D564. *Colloids Surf A Physicochem Eng Asp*. 2009;341:118-126. doi:10.1016/j.colsurfa.2009.03.045
45. Kaftan Ö, Açıkel M, Eroğlu AE, Shahwan T, Artok L, Ni C. Synthesis, characterization and application of a novel sorbent, glucamine-modified MCM-41, for the removal/preconcentration of boron from waters. *Anal Chim Acta*. 2005;547:31-41. doi:10.1016/j.aca.2005.03.043
46. Xu L, Liu Y, Hu H, Wu Z, Chen Q. Synthesis, characterization and application of a novel silica based adsorbent for boron removal. *Desalination*. 2012;294:1-7. doi:10.1016/j.desal.2012.02.030
47. Çelik ZC, Can BZ, Kocakerim MM. Boron removal from aqueous solutions by activated carbon impregnated salicylic acid. *J Hazard Mater*. 2008;152:415-422. doi:10.1016/j.jhazmat.2007.06.120
48. Can BZ, Ceylan Z, Kocakerim MM. Adsorption of boron from aqueous solutions by activated carbon impregnated with salicylic acid: equilibrium, kinetic and thermodynamic studies. *Desalin Water Treat*. 2012;40:69-76. doi:10.1080/19443994.2012.671143
49. Farhat A, Ahmad F, Arafat H. Analytical techniques for boron quantification supporting desalination processes: a review. *Desalination*. 2013;310:9-17. doi:10.1016/j.desal.2011.12.020
50. Alluhaybi AA, Alharbi A, Hameed AM, et al. A novel triazole Schiff Base derivatives for remediation of chromium contamination from tannery waste water. *Molecules*. 2022;27:5087. doi:10.3390/molecules27165087
51. Ibrahium HA, Atia BM, Awwad NS, Nayl AA, Radwan HA, Gado MA. Efficient preparation of phosphazene chitosan derivatives and its applications for the adsorption of molybdenum from spent hydrodesulfurization catalyst. *J Dispers Sci Technol*. 2022;44:2103-2118. doi:10.1080/01932691.2022.2059508
52. Li D, Liu P. Trends and prospects for thermal stabilizers in polyvinyl chloride. *J Vinyl Addit Technol*. 2022;28:669-688. doi:10.1002/vnl.21952
53. Aboghoniem AM, Youssef MA, Darwish OM, Gaballah ST, Rabie ST. Microwave-assisted preparation of fatty acid esters based eco-friendly plasticizers for biologically-active thiazole-functionalized PVC. *J Vinyl Addit Technol*. 2022;28:828-843. doi:10.1002/vnl.21931
54. Gillani QF, Ahmad F, Abdul Mutalib MI, et al. Thermal degradation and pyrolysis analysis of zinc borate reinforced intumescent fire retardant coatings. *Prog Org Coat*. 2018;123:82-98. doi:10.1016/j.porgcoat.2018.05.007
55. Ali H, Silva C, Royer B, Rodrigues Filho G, Cerqueira D, Assunção R. Chemically modified polyvinyl chloride for removal of thionine dye (Lauth's violet). *Materials*. 2017;10:1298. doi:10.3390/ma10111298
56. Jia P, Hu L, Shang Q, Wang R, Zhang M, Zhou Y. Self-plasticization of PVC materials via chemical modification of Mannich base of cardanol butyl ether. *ACS Sustainable Chem Eng*. 2017;5:6665-6673. doi:10.1021/acssuschemeng.7b00900
57. Gao L, Jin D, Lu Y, Xu S. Effects of TiO2@ZnAlSn/PETMP on the properties of plasticized polyvinyl chloride composites. *J Vinyl Addit Technol*. 2022;28:762-774. doi:10.1002/vnl.21919
58. Rusen E, Raluca Ş, Busuioc C, Diacon A. Hydrophilic modification of polyvinyl chloride with polyacrylic acid using ATRP. *RSC Adv*. 2020;10:35692-35700. doi:10.1039/d0ra05936f
59. Delazare T, Ferreira LP, Ribeiro NFP, Souza MMVM, Campos JC, Yokoyama L. Removal of boron from oilfield wastewater via adsorption with synthetic layered double hydroxides. *J Environ Sci Health A*. 2014;49:923.
60. Bilgin SE, Beker U, Senkal BF. Predicting the dynamics and performance of selective polymeric resins in a fixed bed system for boron removal. *Desalination*. 2014;349:39-50. doi:10.1016/j.desal.2014.06.015
61. Zeebe ASRE, Ortiz JD, Wolf-Gladrow DA. A theoretical study of the kinetics of the boric acid–borate equilibrium in seawater. *Mar Chem*. 2001;73:113-124. doi:10.1016/S0304-4203(00)00100-6
62. Ibrahium HA, Abdel Aal MM, Awwad NS, et al. Solid–liquid separation of V(V) from aqueous medium by 3-(2-hydroxy phenyl)-imino-1-phenyl butan-1-one Schiff base immobilized XAD-2 resin. *Int J Environ Sci Technol*. 2022;20:7689-7706. doi:10.1007/s13762-022-04465-5
63. Weshahy AR, Sakr AK, Gouda AA, et al. Selective recovery of cadmium, cobalt, and nickel from spent Ni–Cd batteries using Adogen® 464 and mesoporous silica derivatives. *Int J Mol Sci*. 2022;23:8677. doi:10.3390/ijms23158677
64. Weshahy AR, Gouda AA, Atia BA, et al. Gado MA efficient recovery of rare earth elements and zinc from spent Ni–metal hydride batteries: statistical studies. *Nanomaterials*. 2022;12:2305. doi:10.3390/nano12132305
65. Alharbi A, Gouda AA, Atia BM, Gado MA, Alluhaybi AA, Alkabli J. The role of modified chelating graphene oxide for vanadium separation from its bearing samples. *Russ J Inorgan Chem*. 2022;67:560-575. doi:10.1134/S0036023622040027
66. Langmuir I. The adsorption of gases on plane surfaces of glass, mica and platinum. *Am Chem Soc*. 1918;40:1361-1368.
67. Atia BM, Khawassek YM, Hussein GM, Gado MG, El-Sheify MA, Cheira MF. One-pot synthesis of pyridine dicarboxamide derivative and its application for uranium separation from acidic medium. *J Environ Chem Eng*. 2021;9:105726. doi:10.1016/j.jece.2021.105726
68. Atia BM, Gado MG, Abd El-Magied MO, Elshehy E. Highly efficient extraction of uranyl ions from aqueous solutions using multi-chelators functionalized graphene oxide. *Sep Sci Technol*. 2019;55:2746-2757. doi:10.1080/01496395.2019.1650769
69. Freundlich H. Adsorption in solution. *Phys Chem Soc*. 1906;40:1361.
70. Gado MA, Atia BM, Cheira MF, Elawady ME, Demerdash M. Highly efficient adsorption of uranyl ions using hydroxamic

acid-functionalized graphene oxide. *Radiochim Acta*. 2021;109:743-757. doi:10.1515/ract-2021-1063

71. Ibrahium HA, Awwad NS, Gado MA, Hassanin MA, Nayl AA, Atia BM. Physico-chemical aspects on uranium and molybdenum extraction from aqueous solution by synthesized phosphinimine derivative chelating agent. *J Inorg Organometal Polym Mater*. 2022;32:3640-3657. doi:10.1007/s10904-022-02374-1
72. Atia BM, Sakr AK, Gado MA, et al. Synthesis of a new chelating iminophosphorane derivative (phosphazene) for U(VI) recovery. *Polymers*. 2022;14:1687. doi:10.3390/polym14091687
73. Zarenehad B, Garside J. Crystallization of boric acid through reactive dissolution of oxalic acid crystals in aqueous borax solution. *Devel Chem Eng Miner Process*. 2003;11(5):603-620. doi:10.1002/apj.5500110615
74. Bosi F, Andreozzi GB, Federico M, Graziani G, Lucchesi S. Crystal chemistry of the elbaite-schorl series. *Am Mineral*. 2005;90:1784-1792. doi:10.2138/am.2005.1827
75. Bosi F. Disordering of Fe^{2+} over octahedrally coordinated sites of tourmaline. *Am Mineral*. 2008;93(10):1647-1653. doi:10.2138/am.2008.2722
76. Ning Z-Q, Zhai Y-C, Song Q-S. Extracting B_2O_3 from calcined boron mud using molten sodium hydroxide. *Rare Met*. 2015;34(10):744-775. doi:10.1007/s12598-015-0560-z
77. Zou C, Tang Z, Xie W, et al. Effects of sodium roasting on the leaching rate of boron-bearing tailings and its mechanism analysis. *R Soc Open Sci*. 2018;5:172342. doi:10.1098/rsos.172342
78. Lv X, Ning Z, Zhai Y, Free M, Cui F. Extraction of Si from alkaline-roasted boron ore concentrate. *Iran J Chem Chem Eng*. 2021;40(6):1999. doi:10.30492/IJCCE.2020.118710.3880
79. Duan H, Wang C, Fang Y, et al. Comprehensive utilization of boron-concentrate by hydrometallurgy. *J Sustain Metall*. 2021;7:244-255. doi:10.1007/s40831-020-00328-w
80. Rajadesingu S, Arunachalam KD. Hydration effect of boric acid on the strength of high performance concrete (HPC). *IOP Conf Series Mater Sci Eng A*. 2020;912:062073. doi:10.1088/1757-899X/912/6/062073
81. Wei YT, Zheng YM, Chen JP. Design and fabrication of an innovative and environmental friendly adsorbent for boron removal. *Water Res*. 2011;45:2297-2305. doi:10.1016/j.watres.2011.01.003
82. Wang L, Qi T, Zhang Y. Novel organic–inorganic hybrid mesoporous materials for boron adsorption. *Colloids Surf A Physicochem Eng Aspects*. 2006;275:73-78. doi:10.1016/j.colsurfa.2005.06.075
83. Meng J, Cao J, Xu R, Wang Z, Sun R. Hyper branched grafting enabling simultaneous enhancement of the boric acid uptake and the adsorption rate of a complexing membrane. *J Mater Chem A*. 2016;4:11656-11665. doi:10.1039/c6ta02348g
84. Gazi M, Senakal B, Bicak N. Modification of crosslinked poly(styrene) based polymers for boron–specific extraction. *Macromol Symp*. 2004;217:215-221. doi:10.1002/masy.200451317
85. Wang L, Qi T, Gao Z, Zhang Y, Chu J. Synthesis of N-methylglucamine modified macroporous poly(GMA-co-TRIM) and its performance as a boron sorbent. *React Funct Polym*. 2007;67:202-209. doi:10.1016/j.reactfunctpolym.2006.11.001

SUPPORTING INFORMATION

Additional supporting information can be found online in the Supporting Information section at the end of this article.

How to cite this article: Younis HM, Mohamed AA. A promising modified polyvinyl chloride for adsorption of boron: Preparation, adsorption kinetics, isotherm, and thermodynamic studies. *J Vinyl Addit Technol*. 2023;1-23. doi:10.1002/vnl.22052